Journal of Biomolecular Structure and Dynamics

ISSN: (Print) (Online) Journal homepage: https://www.tandfonline.com/loi/tbsd20

Chemical composition variability and vascular endothelial growth factor receptors inhibitory activity of *Inulaviscosa* essential oils from Algeria

Bouhassane Nadia, Fouzia Mesli, Benomari Fatima Zahra, Nouria Merad-Boussalah, Achiri Radja, Alain Muselli, Nassim Djabou & Mohammed El Amine Dib

To cite this article: Bouhassane Nadia, Fouzia Mesli, Benomari Fatima Zahra, Nouria Merad-Boussalah, Achiri Radja, Alain Muselli, Nassim Djabou & Mohammed El Amine Dib (2022) Chemical composition variability and vascular endothelial growth factor receptors inhibitory activity of *Inulaviscosa* essential oils from Algeria, Journal of Biomolecular Structure and Dynamics, 40:8, 3462-3480, DOI: 10.1080/07391102.2020.1847686

To link to this article: https://doi.org/10.1080/07391102.2020.1847686

JOURNAL OF BIOMOLECULAR STRUCTURE AND DYNAMICS
2022, VOL. 40, NO. 8, 3462–3480
https://doi.org/10.1080/07391102.2020.1847686

Taylor & Francis
Taylor & Francis Group

Chemical composition variability and vascular endothelial growth factor receptors inhibitory activity of *Inulaviscosa* essential oils from Algeria

Bouhassane Nadia[a], Fouzia Mesli[a], Benomari Fatima Zahra[a], Nouria Merad-Boussalah[a], Achiri Radja[a], Alain Muselli[b], Nassim Djabou[c] and Mohammed El Amine Dib[a]

[a]Laboratoire des Substances Naturelles & Bioactives (LASNABIO), Département de Chimie, Faculté des Sciences, Université Abou BekrBelkaıd, Tlemcen, Algeria; [b]Laboratoire Chimie des Produits Naturels, Université de Corse, Corté, France; [c]Laboratoire de Chimie Organique, Substances Naturelles et Analyses (COSNA), Faculté des Sciences, Université Abou BekrBelkaıd, Tlemcen, Algeria

Communicated by Ramaswamy H. Sarma

ABSTRACT

Angiogenes is therefore appears to be a complex phenomenon, finely regulated by various activators (pro-angiogenic factors) and inhibitors (anti-angiogenic factors). Among the pro-angiogenic factors, VEGF (Vascular Endothelial Growth Factor) seems to be one of the main players in tumor angiogenesis. It exerts its pro-angiogenic activity by attaching to the surface of receptors with tyrosine kinase activity (VEGFR). The aim of this research was the bioinformatical study of VEGFR inhibition by essential oils of the Inula viscosa.

Analyses of essential oils obtained by hydrodistillation from the aerial parts of the plant were performed using GC and GC/MS analysis. We used molecular modeling approaches as molecular mechanics to theoretical investigation VEGF receptors by natural inhibitors.

Nineteen compounds were identified, constituting 90.1-98.8% of the total essential oils. The main components of the plants were (E)-nerolidol (15.5–20.2 %), caryophyllene oxide (10.6–18.1%), (E)-Z-farnesyl acetone (13.2–25.1%) and (E)-β-farnesene (1.5–5.6%). Essential oil samples were clustered into two groups according to their chemical compositions. The molecular dynamics study was conducted for the best inhibitors. A few key residues were identified at the binding site of VEGFR. The Pharmacokinetics was justified by means of lipophilicity and high coefficient of skin permeability. The *in silico* evaluation of ADME revealed that L19 has high absorption. The essential oil of *I. viscosa* presents a significant variability. This study revealed that (E)-Z-Farnesylacetone is a functional inhibitor of VEGF activities and subsequently can be the best inhibitors candidate to be scrutinized *in vivo* and *in vitro*.

ARTICLE HISTORY
Received 17 June 2020
Accepted 3 November 2020

KEYWORDS
Inulaviscosa; cancer cells; pharmaco-informatics; molecular dynamic; MOE (molecular operating environment)

1. Introduction

Cancer is a complex disease whose generic term covers different pathologies: There are around 200 types of tumors that can affect all the tissues of the body. In recent years, we have witnessed considerable growth in cancer therapies. Radiotherapy and chemotherapy act mainly against cancer by triggering an overproduction of free radicals in cells (Arruebo et al., 2011). These free radicals constitute reactive oxygen species (ROS). ROS are a family of chemical entities grouping together non-radical derivatives whose toxicity is significant (anion peroxide ($O2^{2-}$), hydrogen peroxide (H_2O_2), peroxynitrite ($ONOO^-$)) and free radicals oxygenate which interests our subject (superoxide anion (O2•−), hydroxyl radical (OH•), alkoxyl radical (RO•), peroxyl radical (ROO•), nitrogen monoxide (NO•), nitric oxide (NO•) and nitrogen dioxide (NO2•)) (Novelli, 1997).These are aggressive molecules, 'carnivores' you could say, which damage cells and can cause their death. But it is an advantage when it comes to cancer cells, which we try to destroy. This is how chemotherapy and radiotherapy act, at least in part, to shrink the size of tumors. The problem is that these therapies do not just target cancer cells. They destroy all the rapidly dividing cells (Lesgards et al., 2014).The study of natural products is one of the strategies for the discovery of new drugs that can be used in cancer therapy. Essential oils have the advantage of being well absorbed by the body. They can be administered in different ways: oral, respiratory (inhalation, olfaction, diffusion), rectal and cutaneous (massage), which gives them great bioavailability (Salim et al., 2017). Numerous *in vitro* studies in mice, rats and hamsters have been carried out to study the effect of essential oils on cancer. A very large number of studies suggest that natural terpenoids like limonene are a new class of anticancer drugs with the ability to cause tumor regression with low toxicity (Lesgards et al., 2014). In addition, numerous studies have also shown that the terpenoids of essential oils could act in synergy with conventional chemotherapy. Antitumor effects have been observed in combination with chemotherapy (Balusamy et al., 2018). For example, the combination of geraniol (essential oil extract)

CONTACT Fouzia Mesli meslifouzia2018@gmail.com; Nouria Merad-Boussalah n.meradbousalah@gmail.com Laboratoire des Substances Naturelles & Bioactives (LASNABIO), Département de Chimie, Faculté des Sciences, Université Abou BekrBelkaıd, BP 119, Tlemcen 13000, Algeria

Supplemental data for this article can be accessed online at https://doi.org/10.1080/07391102.2020.1847686

with 5-fluorouracil (chemotherapy product) reduces the volume of colon cancer in mice by 53%, while chemo alone has no effect and that geraniol alone reduces it by only 26% (Arruebo et al., 2011). *Inulaviscosa* or *Dittrichiaviscosa* belongs to the Asteraceae family. The genus includes more than 90 species distributed in the Mediterranean regions, Spain, France, Asia, Turkey and Africa (Morocco, Egypt and Algeria) (Bouyahya et al., 2018).The viscous inule (*I. viscosa*) contains several secondary metabolites in the aerial parts. It is very rich in volatile compounds (terpenoids) (Bouyahya et al., 2018). The pharmacological properties of *I. viscosa* have been extensively studied. The extracts and essential oils of this plant have shown different pharmacological activities such as anti-inflammatory, antiviral and antitumor activity (Bouyahya et al., 2018). Isocostic acid isolated from the essential oil of *I. viscosa* exhibited an antityrosinase activity comparable to the positive control (kojic acid). Moreover, the calculated bioactivity and drug likeness scores showed also significant binding interaction proven with molecular docking analysis (Aissa et al., 2019). The essential oils from leaves and flowers of *I. viscosa* showed a significant antifungal activity against dermatophytes even at low concentrations (0.01 mg/mL). However, the leaf essential oil exhibited the greatest antifungal efficacy (Cafarchia et al., 2002). The therapeutic effects of this plant have been very diverse and have been known for a long time in traditional medications. It is a plant that is widely used in traditional medicine for its inflammatory, antipyretic and antimicrobial properties (Talib & Mahasneh, 2010). *I. viscosa* is also used to treat gastroduodenal disorders (Al-Dissi et al., 2001; Chahmi et al., 2015) and intestinal disorders. The essential oils are extracted from it for the treatment of various diseases such as bronchitis, diabetes, rheumatism, wounds and diseases of the urinary and digestive system (Al-Dissi et al., 2001; Talib et al., 2012). The study by Rozenblat et al. (2008) revealed the presence of different biologically active sesquiterpenes in *I. viscosa* and their ability to induce apoptosis in cancer cells. Furthermore, modeling and simulation have become standard practices in many scientific and technical fields and in particular in Chemistry. They are often necessary when the real experience is too difficult, too dangerous and too expensive. Computational and theoretical chemistry subsidizes to better comprehension of medicinal plants action against diseases and is being important and crucial to wet laboratory experiment, permitting studying structures and functions of bimolecular (Mesli et al., 2019). To our knowledge, this is the first study that describes the intraspecific variations of essential oils of *I. viscosa* from Algeria from 10 locations using statistical analysis and the structure–activity relationship (SAR). The second objective of this work was to study the essential oils of *I. viscosa* as an inhibitor for VEGF receptors in order to study their mechanism of enzymatic inhibition. Given that vascular endothelial growth factor (VEGF) increases the phosphorylation of tyrosine kinase FAK (Walker, 1996), we set ourselves the goal of inhibiting it in order to decrease phosphorylation. The essential oils of the aerial parts of the *Inulaviscosa* inhibitors were the subject of our investigation. These were used to target the intracellular part of the VEGF receptors (the tyrosine kinase domain), knowing that the two receptors (VEGFR1 and VEGFR2) have different affinities for VEGF and induce different cellular and biological effects. The main interest was to develop new potential inhibitors of the VEGF/VEGFR interaction and finally discuss with the bioactivity scores, drug likeness, pharmacokinetics, medicinal chemistry, molecular docking and molecular dynamics (MD) analysis of major components. The more we know about these interactions, the more we can do with that knowledge. However, many efforts have been made to produce the natural and reliable treatment during the first stage of cancerous cells.

2. Material and methods

2.1. Expiremental procedures

2.1.1. Plant material and essential oil extraction

Plant material used (Aerial parts) of *I. viscosa* was collected at the flowering stage in May 2019 from 10 locations (S1–S10) widespread in the regions of Tlemcen (Algeria) (Table 1). The plant material was botanically authenticated by the Laboratory of Ecology and Ecosystem Management of University of Tlemcen, Algeria. Voucher specimens (see Table 1) were deposited in the herbarium of the Natural and Bioactive Substances Laboratory, Tlemcen University. To obtain essential oils, 400–500 g to aerial parts was subjected to hydrodistillation for a period of 5 h using a Clevenger-type apparatus according to the European Pharmacopoeia. For the chemical analysis, essential oils were stored in dark glass bottles at 4 °C. The essential oil yields were expressed in percent (w/dw) through the weight of dried plant material. The geographical origin, yields and the voucher number of each sample are presented in Table 1.

2.1.2. Analysis conditions

2.1.2.1. Gas chromatography (GC). GC analyses were carried out using a Perkin Elmer Autosystem Clarus 600 GC apparatus (Germany) equipped with a dual flame ionization detection system and fused Rtx-1 silica capillary columns (60 $m \times 0.22$ mm i.d., 0.25-μm film thickness; polydimethylsiloxane). The oven temperature was programmed to increase from 60–230 °C at 2 °C/min and was then held isothermally at 230 °C for 35 min. Injector and detector temperatures were maintained at 280 °C. The essential oils were injected in the split mode (1/50), and the injection volume was 0.2 μL. The retention indices (RI) of the compounds were determined from Perkin Elmer software.

2.1.2.2. Gas chromatography-mass spectrometry (GC-MS). Essential oils were analyzed using a Perkin Elmer Turbo mass detector (quadrupole) coupled to a Perkin Elmer Autosystem XL equipped with Rtx-1 fused silica capillary columns and Rtx-Wax (poly-ethyleneglycol) (ion source temperature, 150 °C; ionization energy, 70 eV). Ionization energy MS were seized over a mass range of 35–350 Da (scan time, 1 s). Other GC conditions were the same as interpreted for GC, except the split was 1/80.

Table 1. Data relative to harvest locations of I. viscosa from Algeria.

Samples	Locations	GPS coordinates	N°. Voucher codes	Yields	Altitudes (m)
S1	SidnaYoucha	35°7′0"N; 1°46′60"O	I.V-0518-DMA7	0.06	5
S2	Beni saf	35°18′8″ N;1°23′1″O	I.V-0518-DMA9	0.08	25
S3	Rachgoun	35°19′26″N; 1°28′47″O	I.V-0518-DMA10	0.06	36
S4	Ghazaouet	35°05′38″N;1°51′37″O	I.V-0518-DMA6	0.05	118
S5	Souahlia	35°1′60″ N; 1°52′60″O	I.V-0518-DMA8	0.1	318
S6	Terny	4°47′45″N; 1°21′29″O	I.V-0518-DMA4	0.09	854
S7	Tlemcen	34°52′41″N; 1°18′53″O	I.V-0518-DMA3	0.08	811
S8	Beni snous	34°38′35″N; 1°33′41″O	I.V-0518-DMA1	0.16	1500
S9	Tafna	34°52′38″N; 1°14′07″O	I.V-0518-DMA2	0.2	1600
S10	EL Aricha	34°13′22″N; 1°15′21″O	I.V-0518-DMA9	0.2	1148

2.1.2.3. Component identification and quantification.

Identification of individual components was accomplished by comparing their GC retention indices (RIs) on nonpolar and polar columns, determined relative to the retention time of a series of n-alkanes with linear interpolation, with those of authentic compounds or literature data (Jennings & Shibamoto, 1980; Joulain & König, 1998; König et al., 2001) and through computer matching with commercial mass spectral libraries (Mc Lafferty & Stauffer, 1988; National Institute of Standards and Technology, 2008) and also by comparing the spectra obtained with those of the in-house laboratory library. The quantification of essential oils and blend was performed using peak normalization (%) abundances calculated by integrating FID response factors relative to tridecane (0.7 g/100 g), used as an internal standard.

3. Theoretical background and comptional details

3.1. Selection of receptor and ligand

In this study, the interactions of essential oils of the aerial parts of *I. viscosa* from compounds as described in Table 2 were investigated. The structures of inhibitors were downloaded from the PubChem database (https://pubchem.ncbi.nlm.nih.gov).

The PDB database (https://www.rcsb.org/) were used to obtain the complete structure of VEGF receptors (VEGFR-1) (PDB ID: **3HNG** [Tresaugues et al., 2013]), VEGFR-2 (PDB ID: **2XIR**), VEGF (PDB ID: **5t89** was obtained by X-ray diffraction).

3.2. Molecular docking

Virtual screening is advised as an alternative method for experimental screening and has a marked up success rate in the drug discovery process. It is a computational analogue of biological screening and has become increasingly popular in the pharmaceutical industry for lead identification (Rasouli et al., 2017). Here, the docking procedure provides specification of the ligand binding site in a receptor and then the docked ligands in the specified site (Rasouli et al., 2017).

3.3. Drug-likeness prediction

Properties analyzed are TPSA, *clogP* calculation, log*S* calculation, molecular weight, fragment based drug-likeness, and drug score (Nisha et al., 2016).

3.4. ADME prediction

ADMET, which constitutes the pharmacokinetic profile of a drug molecule, is very essential in evaluating its pharmacodynamic activities (Nisha et al., 2016). In this study, we have used the SwissADME online property calculation from all these parameters for the best scoring lead compounds (Daina et al., 2017).

3.5. MD simulation

MD aims to numerically simulate condensed phases of a molecular system in order to understand, predict and calculate the properties of a studying system (Champagnat et al., 2013).

The best conformer of VEGF receptors with ligands was subjected to MD simulations was performed for both the complexes (3HNG, 2XIR, 5t89) using the MOE software (Al-Hader et al., 1993). MOE dynamics simulation uses the Nose Poincare-Andersen (NPA) equations of motion (Bond et al., 1999; Sturgeon & Laird, 2000). The Berendsen thermostat is an algorithm to rescale the velocities of particles in MD simulations to control the simulation temperature (Berendsen et al., 1984). The coordinates were stored every 0.2 ps to get an accurate view of molecular movement. In all simulations, the van der Waals cutout distance was set to 8 Å. Energy minimization process was applied by using MMFF94x force field (Parikesit et al., 2015). We have shown the detailed analysis of MD simulation results of only compound L19 with target VEGF receptors (Figures 13–15) because this compound showed better binding affinity for both VEGF receptors. In the end and according to the MD simulation analysis among these two compounds, the most active compounds were L4 and L19 in VEGF receptors.

4. Results and discussion

4.1. Experimental

4.1.1. Yields and chemical compositions of I. viscosa essential oils

The hydrodistillation of dry leaves of *I. viscosa* of different stations led to the isolation of yellowish oils. The essential oil yields of populations, collected from study areas, are shown in Table 1. Essential oil yields varied from 0.05% to 0.2% (w/w), among stations. The highest yields of essential oils were obtained in the stations of Tafna (0.2%) (S9), EL Aricha (0.2%) (S10) and Beni snous (0.16%) (S8), with altitudes above 1000 m, while the lowest (0.05%–0.1%) were observed in the

Table 2. Various drugs used in the *in silico* docking studies. 'Adopted from online PubChem database (accessed on 07.01.2014). Adoptedfrom online CHEMBL database (accessed on 13.11.2013)'.

No.	Anti-angiogenic drug	IUPAC Name	CID/ N°	M.W. (g/mol)	Molecular Formula	Structure
1	cis-α-Bergamotene	(1S,5S,6S)-2,6-dimethyl-6-(4-methylpent-3-enyl)bicyclo[3.1.1]hept-2-ene	**6429303**	204.35	$C_{15}H_{24}$	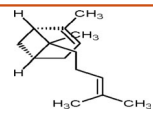
2	(*E*)-β-Caryophyllene	[(5Z)-6,10-dimethyl-2-methylidene-10-bicyclo[7.2.0]undec-5-enyl]methanol	**5352484**	220.35	$C_{15}H_{24}O$	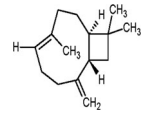
3	β-Copaene	1,3-dimethyl-8-propan-2-yltricyclo[4.4.0.02,7]dec-3-ene	**19725**	204.35	$C_{15}H_{24}$	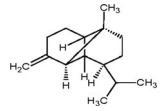
4		(3E,6E)-3,7,11-trimethyldodeca-**1,3,6,10**-tetraene	**5281516**	204.35	$C_{15}H_{24}$	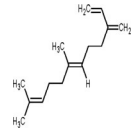
5	allo-Aromadendrene	(4aS,7R,7aR)-1,1,7-trimethyl-4-methylidene-2,3,4a,5,6,7,7a,7b-octahydro-1aH-cyclopropa[e]azulene	**42608158**	204.35	$C_{15}H_{24}$	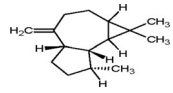
6	Germacrene-D	(1Z,6Z,8S)-1-methyl-5-methylidene-8-propan-2-ylcyclodeca-1,6-diene	91723653	204.35	$C_{15}H_{24}$	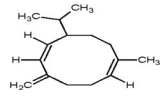
7	Zingibrene	(5R)-2-methyl-5-[(2S)-6-methylhept-5-en-2-yl]cyclohexa-1,3-diene	92776	204.35	$C_{15}H_{24}$	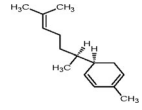
8	Bicyclogermacrene	(1R,2E,6E,10S)-**3,7,11,11**-tetramethylbicyclo[8.1.0]undeca-2,6-diene	11820258	204.35	$C_{15}H_{24}$	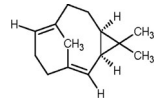
9	γ-Cadinene	(1S,8aR)-4,7-dimethyl-1-propan-2-yl-**1,2,3,5,6,8**a-hexahydronaphthalene	441005	204.35	$C_{15}H_{24}$	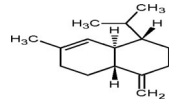
10	δ-Cadinene	(1S,4aR,8aR)-7-methyl-4-methylidene-1-propan-2-yl-2,3,4a,5,6,8a-hexahydro-1H-naphthalene	6432404	204.35	C15H24	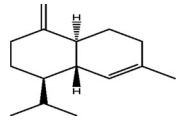
11	(*E*)-Nerolidol	(6E)-3,7,11-trimethyldodeca-1,6,10-trien-3-ol	5284507	222.37	$C_{15}H_{26}O$	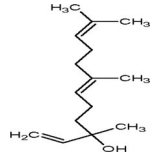
12	Caryophyllene oxide	(1R,4R,6R,10S)-4,12,12-trimethyl-9-methylidene-5-oxatricyclo[8.2.0.04,6]dodecane	1742210	220.35	$C_{15}H_{24}O$	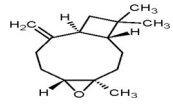
13	Globulol	(1aR,4R,4aR,7R,7aS,7bS)-1,1,4,7-tetramethyl-2,3,4a,5,6,7,7a,7b-octahydro-1aH-cyclopropa[e]azulen-4-ol	12304985	222.37	$C_{15}H_{26}O$	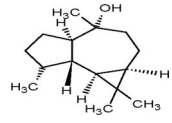

(*continued*)

Table 2. Continued.

No.	Anti-angiogenic drug	IUPAC Name	CID/ N°	M.W. (g/mol)	Molecular Formula	Structure
14	Ledol	(1aR,4R,4aS,7R,7aS,7bS)-1,1,4,7-tetramethyl-2,3,4a,5,6,7,7a,7b-octahydro-1aH-cyclopropa[e]azulen-4-ol	92812	222.37	$C_{15}H_{26}O$	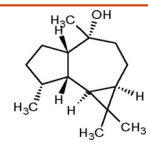
15	Zingibereol	1-methyl-4-(6-methylhept-5-en-2-yl)cyclohex-2-en-1-ol	13213649	222.37	$C_{15}H_{26}O$	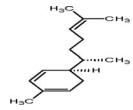
16	τ-Muurolol	(1S,4S,4aR,8aS)-1,6-dimethyl-4-propan-2-yl-3,4,4a,7,8,8a-hexahydro-2H-naphthalen-1-ol	3084331	222.37	$C_{15}H_{26}O$	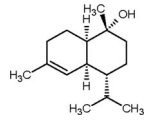
17	α-Cadinol	(1R,4S,4aS,8aS)-1,6-dimethyl-4-propan-2-yl-3,4,4a,7,8,8a-hexahydro-2H-naphthalen-1-ol	12302222	222.37	$C_{15}H_{26}O$	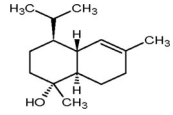
18	α-Bisabolol	(2R)-6-methyl-2-[(1R)-4-methylcyclohex-3-en-1-yl]hept-5-en-2-ol	1549992	222.37	$C_{15}H_{26}O$	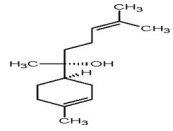
19	Farnesylacetone	(5E,9E)-6,10,14-trimethylpentadeca-5,9,13-trien-2-one	1711945	222.37	$C_{18}H_{30}O$	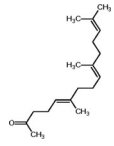

stations S1 to S7 with altitudes varying from 5 to 854 m. The chemical composition analysis *I. viscosa* essential oils of 10 stations (Table 3) allowed the identification of 19 compounds, accounting for 90.1%–98.8% of oils.

All components were identified by comparing their mass spectra (EI-MS) and retention indices (RIs) with those of mass spectral library, 10 sesquiterpene hydrocarbons and 9 oxygenated sesquiterpenes were identified (Table 3). The EO Coll of *I. viscosa* showed only the presence of sesquiterpenes compounds (97.2%). The oxygenated sesquiterpenes were the most dominant with a percentage of 87.3%. The major components were α-bisabolol (16.0%), (*E*)-Z-farnesylacetone (13.2%), (*E*)-nerolidol (15.5%), α-cadinol (11.6%), caryophyllene oxide (10.6%) and τ-muurolol (9.8%), while the sesquiterpene hydrocarbons were represented by small amounts of (*E*)-β-farnesene (2.6%), allo-aromadendrene (1.8%) and δ-cadinene (1.5%) (Table 3).When we compare our data, with those in the literature, it appears that the chemical composition of our oil is markedly different from other regions of the word. Indeed, the major components of essential oil of Turkey were borneol (25.2%), isobornylacetate (22.5%) and bornyl acetate (19.5%) (Pérez-Alonso et al., 1996), that of France and Spain was fokienol (21.1% and 38.8%, respectively) (Blanc et al., 2006; Camacho et al., 2000), while that of Jordan were fokienol (20.9%) and (E)-nerolidol (19.8%) (Al-Qudah et al., 2010). While Eudesma-3,11(13)-dien-12-oic acid was detected as main constituent in *I. viscosa* essential oil from the East Algeria (56.8%) and southern Italy (62.4%) (De Laurentis et al., 2002; Haoui et al., 2015), on the other hand, δ-terpinène (35.9%) and α-pinène (18.9%) were the major components of essential oil of Sidi Bel Abbes (Algeria) (Benchohra et al., 2011). 3-methoxy cuminylisobutyrate (12%) and α-cadinol (6.3%) dominate the composition of Portugal *I. viscosa* essential oils. The composition of the Tunisian *I. viscosa* leaves essential oil was characterized by high oxygenated sesquiterpenes (92.7%) dominated by isocostic acid (70.8%) (Aissa et al., 2019). Various studies on the essential oil of *I. viscosa* reported the presence of globulol (26, 15.0%), chamazulene (27, 49.6%) and 1,4-dimethylazulene (28, 32.1%) in high percentage (Chiarlo, 1968). On the other hand, the leaves contained the eucalyptol (Lauro & Rolih, 1990).

4.2. Chemical variability of essential oils

However, quantitative differences were greatly observed in the major essential oil constituents of different stations (S1–S10) due their geographic location. Indeed, the cluster analysis according to (CA) (Figure 1) the main compounds (N° 11,12, 16–19 of Table 3) showed significant differences. The dendrogram (CA) was obtained using the nearest neighbor method; it suggests that there were two main groups of *I. viscosa* oils (Figure 1). The first group (I) included oil samples from five localities (S1–S5). The second group (II) constituted of samples from five localities (S6–S10). The second

Table 3. Chemical composition of essential oils of the aerial parts of *I. viscosa* collected in 10 stations in the North West of Algeria.

No.[a]	Components	RI[b]	RI[c]	RI$_p$[d]	EO Coll	S1	S2	S3	S4	S5	S6	S7	S8	S9	S10	Identification[e]
1	cis-α-Bergamotene	1411	1409	1560	0.9	1.2	1.2	0.6	0.2	0.1	1.2	1.1	0.1	1.5	1.6	RI, MS
2	(*E*)-β-Caryophyllene	1421	1418	1590	0.3	0.3	0.2	0.6	1.5	1.8	0.3	0.2	0.6	1.2	0.3	RI, MS
3	β-Copaene	1431	1430	1579	0.8	0.4	0.5	0.1	0.6	0.3	0.1	0.1	0.4	0.3	0.1	RI, MS
4	(*E*)-β-Farnesene	1448	1444	1660	2.6	1.6	3.2	4.8	5.6	2.6	0.3	0.5	0.6	0.3	0.5	RI, MS
5	allo-Aromadendrene	1462	1459	1637	1.8	1.3	0.8	2.3	3.3	0.3	0.5	0.6	1.3	1.1	0.9	RI, MS
6	Germacrene-D	1480	1477	1700	0.5	0.8	1.5	1.1	0.6	0.9	0.5	0.3	0.1	0.1	0.1	RI, MS
7	Zingibrene	1489	1486	1715	0.1	0.4	0.5	0.1	0.1	0.3	0.8	0.2	0.1	0.1	0.1	RI, MS
8	Bicyclogermacrene	1494	1492	1720	0.5	0.3	0.6	0.2	0.1	0.5	1.3	0.2	0.3	0.2	0.1	RI, MS
9	γ-Cadinene	1507	1509	1752	0.9	1.1	0.9	2.1	0.1	0.6	1.4	0.2	0.1	0.8	0.2	RI, MS
10	δ-Cadinene	1516	1522	1785	1.5	0.8	0.2	0.6	0.3	1.3	6.3	0.3	0.1	0.7	0.1	RI, MS
11	(*E*)-Nerolidol	1546	1551	2036	15.5	30.2	20.5	19.5	20.5	18.3	5.3	4.2	4.8	3.2	5.2	RI, MS
12	Caryophyllene oxide	1576	1569	1985	10.6	13.6	12.3	15.6	18.1	11.8	5.8	5.1	6.5	3.5	7.3	RI, MS
13	Globulol	1589	1581	2066	2.9	2.3	1.3	2.3	2.9	5.3	5.3	6.9	7.2	9.1	7.3	RI, MS
14	Ledol	1600	1605	2023	4.5	2.5	7.6	7.5	1.5	3.9	3.5	3.1	5.4	3.7	0.7	RI, MS
15	Zingiberenol	1613	1612	2169	3.2	7.3	1.8	2.6	2.3	6.5	1.6	8.5	4.3	3.5	0.5	RI, MS
16	τ-Muurolol	1634	1631	2142	9.8	0.3	5.7	0.6	0.2	0.1	10.5	14.5	25.3	29.5	33.2	RI, MS
17	α-Cadinol	1645	1641	2108	11.6	8.1	9.2	7.5	5.5	10.3	25.3	26.3	19.5	20.1	18.6	RI, MS
18	α-Bisabolol	1672	1671	2216	16.0	3.1	5.6	4.1	1.6	6.6	26.2	22.3	15.3	17.3	16.3	RI, MS
19	(*E*)-Z-Farnesylacetone	1871	1879	2331	13.2	23.2	19.6	18.5	25.1	21.6	2.6	2.2	1.1	0.6	2.3	RI, MS
% **Identification**					**97.2**	**98.8**	**93.2**	**90.7**	**90.1**	**93.1**	**98.8**	**96.8**	**93.1**	**96.8**	**95.4**	
Sesquiterpene hydrocarbons					9.9	8.2	9.6	12.5	12.4	8.7	12.7	3.7	3.7	6.3	4.0	
Oxygenated sesquiterpenes					87.3	90.6	83.6	78.2	77.7	84.4	86.1	93.1	89.4	90.5	91.4	

[a]Order of elution is given on apolar column (Rtx-1).
[b]Retention indices of literature on the apolar column (RILit).
[c]Retention indices on the apolar Rtx-1 column (RIa).
[d]Retention indices on the polar Rtx-wax column (RIp).
[e]RI: Retention Indices; MS: Mass Spectra in EI mode.

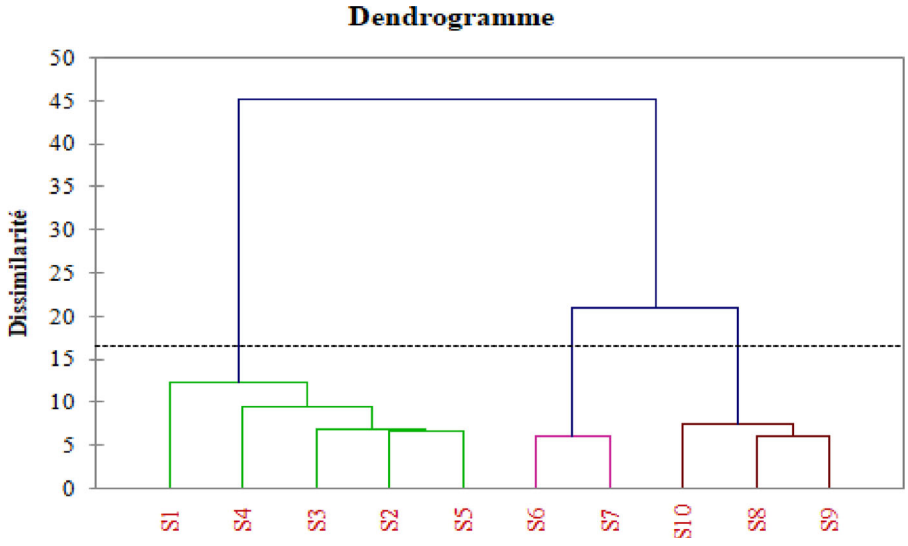

Figure 1. Cluster analysis (CA) of chemical compositions of essential oil of *I. viscosa* from the North West of Algeria.

group was characterized by two subgroups. The subgroup (I1) contained the stations S6 and S7 and the subgroup (I2), the stations S8–S10.

Principle component analysis (PCA) (Figure 2) shows the relationships between family of compounds and geographic location. The first two PCA axes accounted for 82.96% and 8.5% of the total variance, respectively.

The results of PCA highly confirmed the existence of two main groups. Group I (S1–S5) at low altitude was mainly discriminated by the contents of (E)-nerolidol (15.5%–20.2%), caryophyllene oxide (10.6%–18.1%), (E)-Z-farnesylacetone (13.2%–25.1%) and (E)-β-farnesene (1.5%–5.6%). On the other hand, stations S6 and S7 (subgroup I1) were characterized by the presence of a higher percentage of α-bisabolol (25.3% and 26.3%, respectively) and α-cadinol (25.3% and 26.3%, respectively), compared to other stations, while the subgroup I2 (S8–S10) with higher altitudes (1148–1600 m) was richer by τ-muurolol (25.3%–33.2%) and globulol (7.2%–9.1%) (Figure 2, Table 3). However, the observed differences in the chemical composition of essential oils can be justified by many factors such as abiotic stresses (Belabbes et al., 2017), the cultivation area, collected material, altitude and age of the plant (Ma et al., 2019). Sesquiterpenes were the most distinct group in terms of the structure of the terpenoids, most of which exert biological activities (Hou et al., 2014; Khana et al., 2008) and have been reported to be active against the

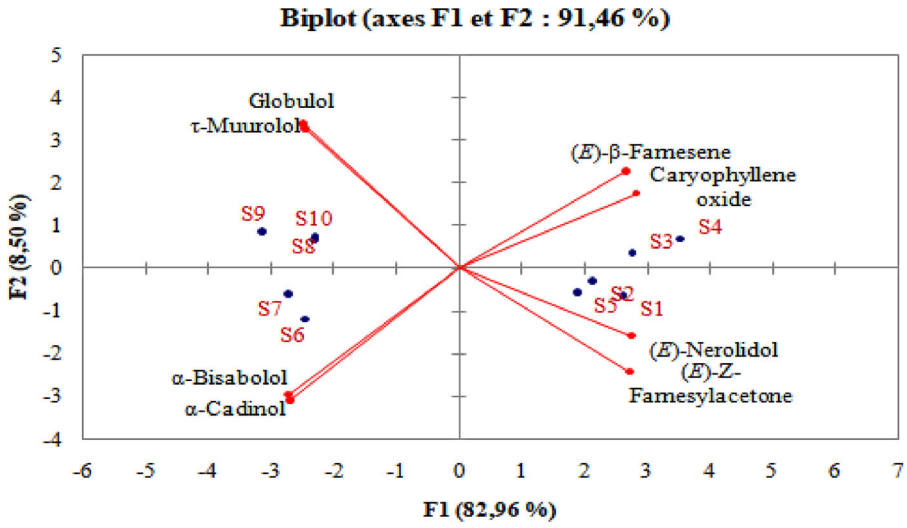

Figure 2. PCA of chemical compositions of essential oils of *I.viscosa*. Distribution of variables.

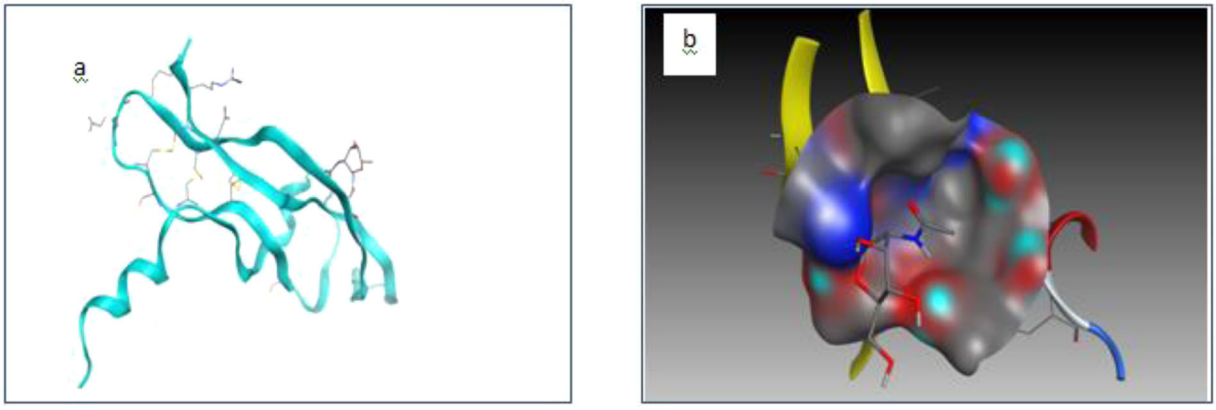

Figure 3. (a) Simplified model of (VEGF). (**b**) The active site of the isolated VEGF.

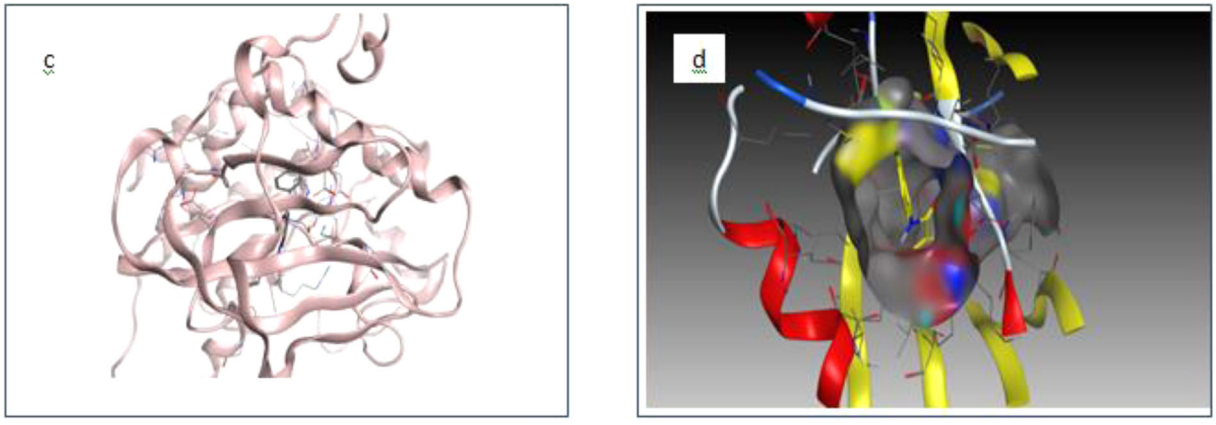

Figure 4. (c) Simplified model of (VEGFR-1 receptor). (d) The active site of the isolated VEGFR-1.

oxidative stress (Su et al., 2015), β-caryophyllene, τ-muurolol, α-cadinol and (2Z,6E)-farnesol exhibit cytotoxic activity against human colon, liver and lung cancer cells (Cavalieri et al., 2004). α-bisabolol was found to have a strong time- and dose-dependent cytotoxic effect on human and rat glioma cells (Cavalieri et al., 2004).

4.2.1. Theoretical

The enzyme's active sites with co-crystallization molecule are shown in Figures 3–5.

The ligands of essential oils of the aerial parts of *I. viscosa* minimized toxicity, and energy obtained by MOE software is shown in Table 4.

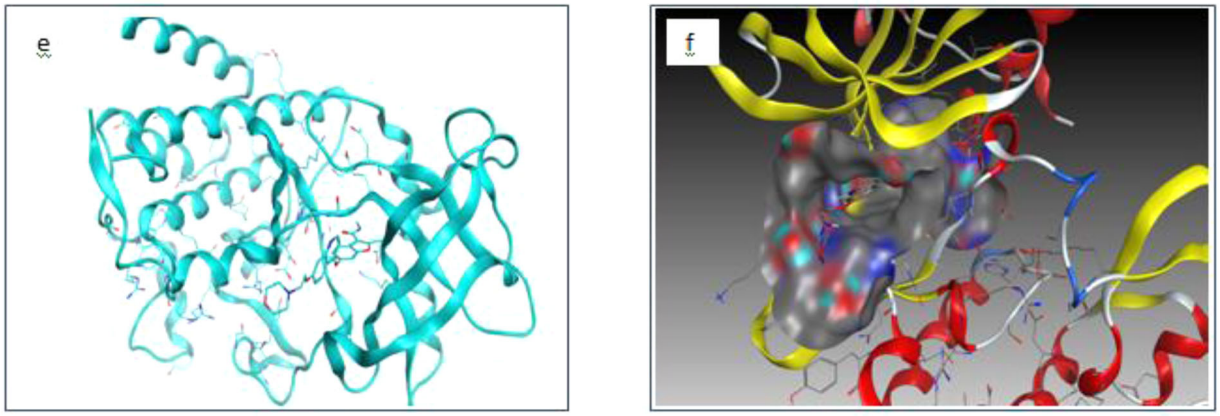

Figure 5. (e) Simplified model of (VEGFR-2 receptor). (f) The active site of the isolated VEGFR-2.

Table 4. Minimization energy of molecules natural for anti-angiogenic drug (kcal/mol).

Ligand	Molecules	Energies(Kcal/mol)	LogP	LogS	Toxicity
1	cis-α-Bergamotene	3.91656e + 001	4.73	−5.29	No
2	(*E*)-β-Caryophyllene	4.00404e + 001	3.70	−3.07	No
3	β-Copaene	4.34100e + 001	4.27	−5.91	No
4	(*E*)-β-Farnesene	2.18401e + 001	5.20	−6.01	No
5	allo-Aromadendrene	5.36129e + 001	4.27	−6.41	No
6	Germacrene-D	3.17611e + 001	4.89	−4.74	No
7	Zingibrene	2.59488e + 001	4.89	−4.87	No
8	Bicyclogermacrene	4.80650e + 001	4.73	−4.67	No
9	γ-Cadinene	2.61312e + 001	4.73	−4.80	No
10	δ-Cadinene	2.95608e + 001	4.58	−5.17	No
11	(*E*)-Nerolidol	2.19630e + 001	4.40	−3.93	No
12	Caryophyllene oxide	4.51752e + 001	3.94	−4.39	Yes
13	Globulol	5.49887e + 001	3.47	−4.79	No
14	Ledol	5.91711e + 001	3.47	−4.79	No
15	Zingibereol	2.38235e + 001	4.09	−4.37	No
16	τ-Muurolol	3.54879e + 001	3.78	−3.54	No
17	α-Cadinol	3.89123e + 001	3.78	−3.54	No
18	α-Bisabolol	2.58813e + 001	4.23	−2.92	No
19	(*E*)-Z-Farnesylacetone	2.17939e + 001	5.77	−5.18	No

These ligands are capable of providing crucial biological activities in accordance with the principle of Lipinski et al. (1997) (Petersson et al., 1988).

As stated in the table above, we find that the molecules L19 and L4 have a high value of Log P and Log S compared to other molecules and also, the results obtained show that these ligands (L19 and L4) have a high value of torsion angle relative to other compounds. This shows that these compounds are more flexible. In addition, it is noted that the growth of the torsion angle depends on the binding number of the molecule. The information of all compounds was obtained from MOE software (Molecular Operating Environment (MOE), 2013.08, 2016).

4.3. Molecular docking

4.3.1. Natural inhibitor approach

4.3.1.1. VEGF. We note that the result obtained (Table 5), out of the best compounds studied, Farnesylacetone (Ligand 19) (Figure 6) was predicted to be the strongest VEGF receptor binder that forms a complex with the most stability with the lowest energy −4.52469969Kcal/mol. The ligands that interacted withVEGFR-1 were as follows: Ligand L2 interacted with two amino acids (GLU 93 and GLU 93) at a distance of 2.51, 2.82 Å strong with energy of 1.2 and −1.0, respectively, and ligand L11 interacts with one amino acid GLU 38 H – donor at a distance of 2.58 Å strong and energy binding of −1.4; similarly, the ligand L12 interacted with one amino acid LEU 97 H-acceptor at a distance of 2.96 Å. It is noted that the interactions between the residue of the active site of 5t89 and Farnesylacetone ligand formed a stable complex.

The second best binder was (*E*)-β-Farnesene (Ligand 4) (Figure 7) with the energy of −4.01963854 Kcal/mol. This suggests that (*E*)-β-Farnesene can inhibit VEGF receptors.

4.3.1.2. VEGFR-1. We note that Farnesyl acetone (Ligand 19) (Figure 8) was predicted to be the strongest VEGF receptor binder that formed a complex with the most stability and the lowest energy (−4.52469969 Kcal/mol) that interacted with two amino acids (ARG 1021 and ARG 1021) H-acceptor at a distance of interaction of 3.00 and 2.94 Å, respectively, with the existence of eight electric forces (GLU910, GLU 878, CYS 912, VAL 891, LEU 882, ASP1040, LYS861 and ARG1021). The existence of electric force suggests that Farnesylacetone can inhibit VEGF receptors. It is noted that the interactions between the residues of the active site of 3HNG and the Farnesylacetone ligand form a stable complex with a strong interaction.

The second best binder was (*E*)-β-Farnesene(Ligand 4) (Figure 9) with the energy of –7.55429745 Kcal/mol. The ligands that interacted with VEGFR-1 were as follows: Ligand L3 interacted with a one amino acid PHE 1041 H-pi at a distance of 4.08 Å, low interaction with energy binding of −0.7, and then, Ligand L14 interacted with two amino acids GLU910 and CYS912 H-donor and H-acceptor, respectively, with energy of 1.8 and 1.7, respectively. Lastly, the ligand L19 interacted with same amino acids ARG 1021 H-acceptor with energy between receptor and amino acids were −4.5 and −1.6, respectively (See supplementary Figures 16–18).

4.3.1.3. VEGFR-2. We note that Farnesylacetone (Ligand 19) (Figure 10) was predicted to be the strongest VEGF receptor binder that formed a complex with the most stability with the lowest energy −8.10823059 Kcal/mol) with the existence of four electric force (GLU 917, CYS 919, ASP 1024 and LEU 840). This suggests that Farnesylacetone can inhibit VEGF receptors. It is noted that the interactions between the

Table 5. Energy balance of complexes formed with anti-angiogenic drug without water molecules (Kcal/mol).

Mol	Pose	Score	Rmsd–refine	E-Conf	E- PLACE	E-REFINE	RMSD
Lref1 (Native)	10	−3.78999758	3.80355144	53.460392	−42.1670952	−9.73435974	1.428
VEGF							
L1	3	−3.49325585	1.4171623	49.4205856	−9.02826786	−9.28911781	1.385
L2	6	−3.54622912	4.25287771	45.9673691	−22.3249168	−9.67628956	0.394
L3	2	−3.38240385	1.97325587	49.2433662	−18.0179806	−7.8158865	0.298
L4	5	−4.01963854	1.95341456	34.3210564	−15.5851097	−9.65795422	1.447
L5	5	−3.38378692	2.55735159	71.8157883	−24.9921379	−8.56387329	0.111
L6	7	−3.18338823	1.66500854	40.1790848	−25.3914356	−7.22984791	0.570
L7	2	−3.73947215	1.08847892	37.5174332	−37.0030251	−10.5696306	0.197
L8	3	−3.52705669	2.08294535	61.8202896	−16.5464706	−9.45939064	0.198
L9	4	−3.69257712	2.31939769	43.0718536	−25.7758541	−9.50582314	0.343
L10	4	−3.45229697	3.45120263	11.3685236	−1.34288752	−8.6183157	0.079
L11	8	−3.98458982	1.67662919	32.5299606	−34.1233177	−12.5704956	0.211
L12	5	−3.59765863	3.55976343	13.6160984	5.93009233	−9.25728226	0.215
L13	8	−3.80335522	6.73355961	13.5810099	−22.7992706	−10.0778494	0.263
L14	8	−3.75419545	2.29156828	62.2090683	−20.9349194	−9.60580826	0.139
L15	6	−3.60531759	1.56402004	22.7498188	−24.3484097	−8.58475876	0.081
L16	7	−3.23660111	3.0124259	38.370285	−12.1734447	−7.70761824	0.197
L17	8	−3.55800462	2.01988792	40.3355331	−39.8503456	−9.25317478	0.087
L18	6	−3.71103525	1.1156019	32.8649559	−28.2323246	−10.1320171	0.320
L19	9	−4.52469969	1.46585608	38.5425644	−34.7141495	−12.7509823	0.053
Mol	**Pose**	**Score**	**Rmsd–refine**	**E-Conf**	**E-PLACE**	**E-REFINE**	**RMSD**
Lref2	6	−10.2159939	1.63261998	47.5232811	−84.9253769	−33.8748169	0.659
RESPTOR1/ VEGFR1							
L1	5	−5.67572975	0.738956094	55.8443031	−58.5605888	−3.56594133	0.814
L2	9	−5.79094362	1.84575272	49.6417389	−62.4633102	−16.9630489	0.673
L3	8	−5.31909132	2.69288158	50.999691	−52.446312	−14.2888889	0.242
L4	8	−7.55429745	1.32448125	39.0443153	−66.0409241	−20.4006729	1.143
L5	8	−5.51163673	3.15417051	72.1863174	−57.3297005	−16.5133209	0.115
L6	7	−5.51596737	1.31669843	42.5609818	−58.9852829	−12.8108568	0.250
L7	10	−6.2743659	1.10227025	36.787323	−54.5825882	−19.3177948	0.035
L8	4	−4.31459522	1.23091698	66.5092773	−45.724987	0.929653227	0.485
L9	7	−5.35120869	2.12681007	46.9883537	−54.7862587	−10.063139	0.433
L10	9	−5.29777861	0.688894331	15.5641155	−51.1675949	−10.7363739	0.420
L11	10	−6.78250837	1.8873719	41.0823135	−52.1711159	−13.4837017	0.502
L12	7	−5.14908934	1.49792802	16.2355289	−53.7675209	−10.9783001	0.356
L13	8	−4.79661131	1.32344747	15.2820148	−59.1631584	−10.7241364	0.366
L14	7	−5.34053659	2.14731693	63.0932159	−51.9754829	−14.3296251	0.268
L15	9	−5.08465052	2.31756425	24.4453144	−60.2406654	−15.4020233	0.444
L16	9	−5.04594994	0.91354239	39.0615311	−49.6845665	−12.8063755	0.023
L17	10	−4.74857521	1.52684665	−52.9785118	−52.9785118	−12.808341	0.416
L18	10	−5.1971302	2.11682534	30.7944088	−69.2757645	−15.7095633	0.413
L19	10	−7.96668291	2.71927118	39.4914207	−58.6933594	−22.9831047	0.492
RECEPTOR2/ VEGFR2							
Mol	**Pose**	**Score**	**Rmsd–refine**	**E-Conf**	**E-PLACE**	**E-REFINE**	**RMSD**
Lref3	10	−10.4227104	2.93172359	35.6387901	−67.0485001	−16.9801006	0.891
L1	4	−4.71330452	1.21814144	59.5516663	−50.5476265	3.48999476	0.354
L2	8	−5.82724428	1.41441953	61.5446854	−58.9625435	−10.2989044	0.326
L3	9	−5.65643024	2.08355451	50.0475235	−51.9137001	−15.2227755	0.261
L4	5	−7.39465475	1.14210582	44.2986488	−63.8447723	−14.1900234	1.425
L5	7	−4.11897755	1.77988875	84.4658127	−46.6783981	8.42493057	0.232
L6	9	−5.33562517	3.33458853	42.0842743	−51.0991707	−11.4472246	0.160
L7	10	−6.07355309	1.99330485	43.4474983	−53.7330627	−7.46748018	0.489
L8	8	−5.7500782	1.74556887	64.2186813	−48.4922371	−14.2425623	0.360
L9	10	−5.50285721	1.36944818	45.387619	−46.9052887	−14.3059397	0.400
L10	8	−5.40128326	2.46785975	19.8633728	−55.3035316	−9.68788242	0.261
L11	9	−6.50306749	1.21159434	37.4934464	−41.4966698	−4.83200741	0.433
L12	7	−5.50666094	1.6465497	15.9660406	−45.2692986	15.9660406	0.506
L13	9	−5.69354916	1.88015425	14.4716063	−55.745636	−11.8592186	0.264
L14	6	−5.68339872	2.26530838	62.3576508	−59.3398705	−16.6589127	0.240
L15	10	−5.73431635	1.14088261	39.3782997	−51.5355682	−5.62705517	0.429
L16	9	−5.5116353	1.2355634	−55.0190964	−55.0190964	−16.762455	0.278
L17	6	1.13416386	1.97636449	73.7940826	−59.6460381	65.2220993	0.434
L18	8	−6.22930002	0.602132857	43.9919434	−65.4302063	5.66625738	0.395
L19	8	−8.10823059	1.78886366	47.4458733	−87.4332504	−21.52174	0.557

residue of the active site of 2XIR and the Farnesylacetone ligand form a stable complex with a strong interaction.

The second best binder was (*E*)-β-Farnesene (Ligand 4) (Figure 11) with the energy of −7.39465475 Kcal/mol (Table 5), with the existence of four electric force (GLU 917, CYS 919, LEU 840 and ASP 1046). This suggests that (*E*)-β-Farnesene can inhibit VEGF receptors. The ligands that interact withVEGFR-2 were as follows: Ligand 1 interacts with one amino acid PHE 1041 H-pi at a distance of 4.44 Å, low interaction with energy binding of −0.7. Then, Ligand L16 interacts with two amino

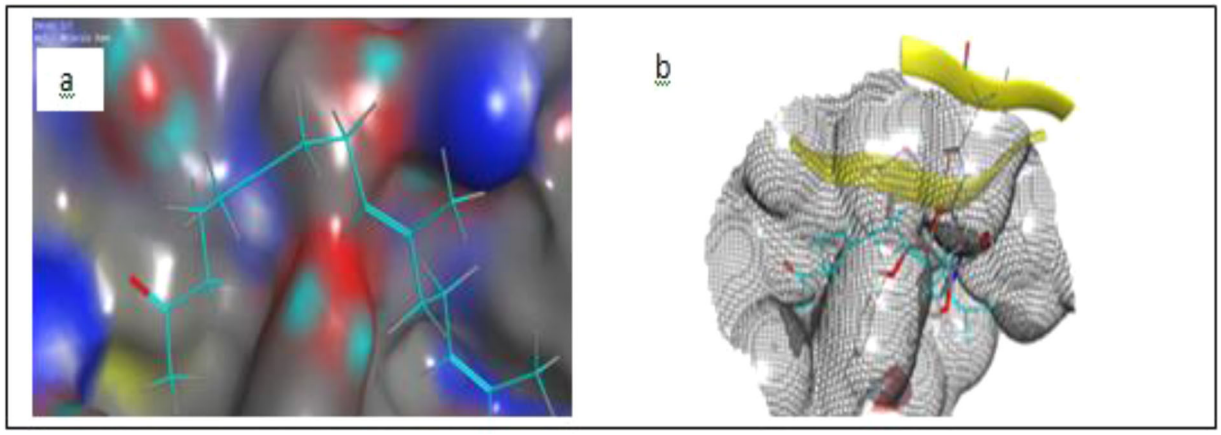

Figure 6. (a) The top scoring compound. (b) A novel inhibitor L-19 identified by molecular docking Farnesylacetoneis shown in the active site.

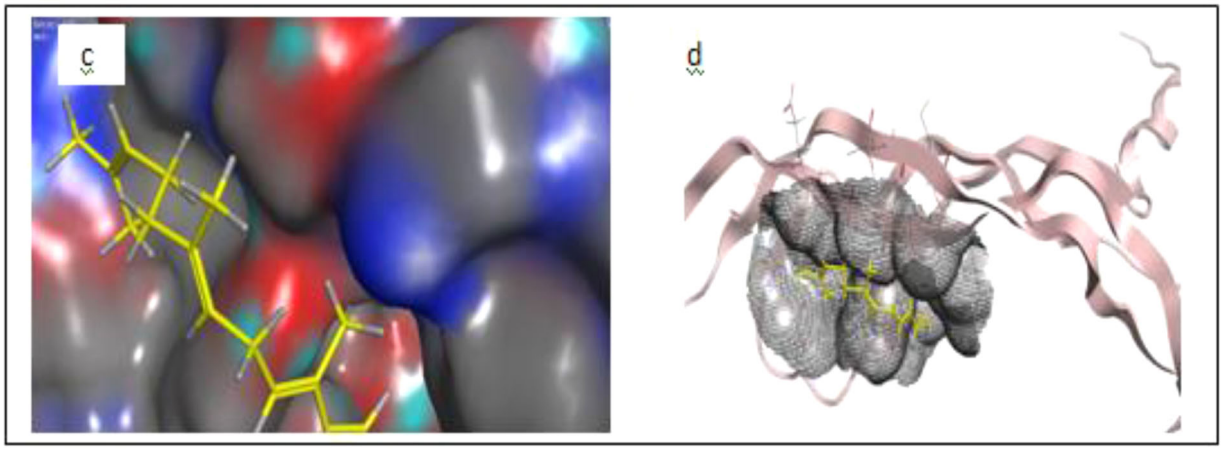

Figure 7. (c) The top scoring compound. (d) A novel inhibitor L-4 identified by molecular docking (*E*)-β-Farneseneis shown in the active site.

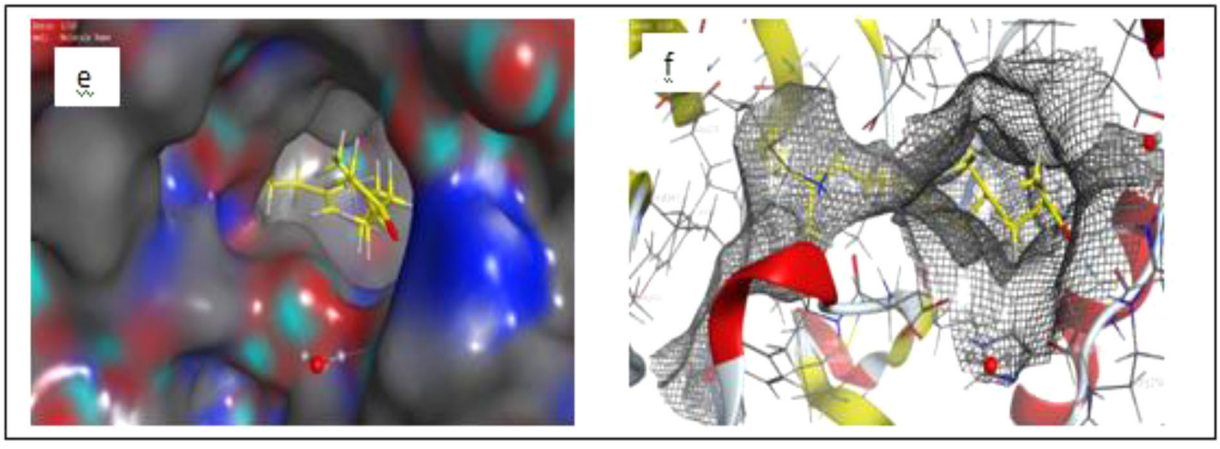

Figure 8. (e) The top scoring compound. (f) A novel inhibitor L-19 identified by molecular docking Farnesylacetone is shown in the active site.

acids HOH 3159 and ASN 923H-donor and H-acceptor, respectively, with energy of 0.5 and −0.5 at distance of 2.51 and 3.26, respectively. Also quote, Ligand L11 defined by strong interaction at distance of 2.95 Å and interaction binding energy of −0.8 with one amino acid ASP 1046 H-donor. Lastly, the Ligand L18 interacts with one amino acid PHE 1047H-pi with energy between receptor and amino acids is –0.6. Results of 19 compound bonds between atoms of compounds and residues of the active site are given in Table 6.

4.3.2. VEGF–VEGFR interaction

The two VEGF monomers participate in the interaction with the d2 domain of VEGFR1 (Figure 12). The results of docking energies of VEGF/VEGFR inhibitors are shown in Table 7.

Treatments targeting VEGF can have direct effects on the tumor cell (strain). The ligand is designated as the best inhibitor and forms a stable complex.The ligand (E)-Z-Farnesylacetone L19 was able to replace ATP, thereby preventing phosphorylation activity. We can conclude that for

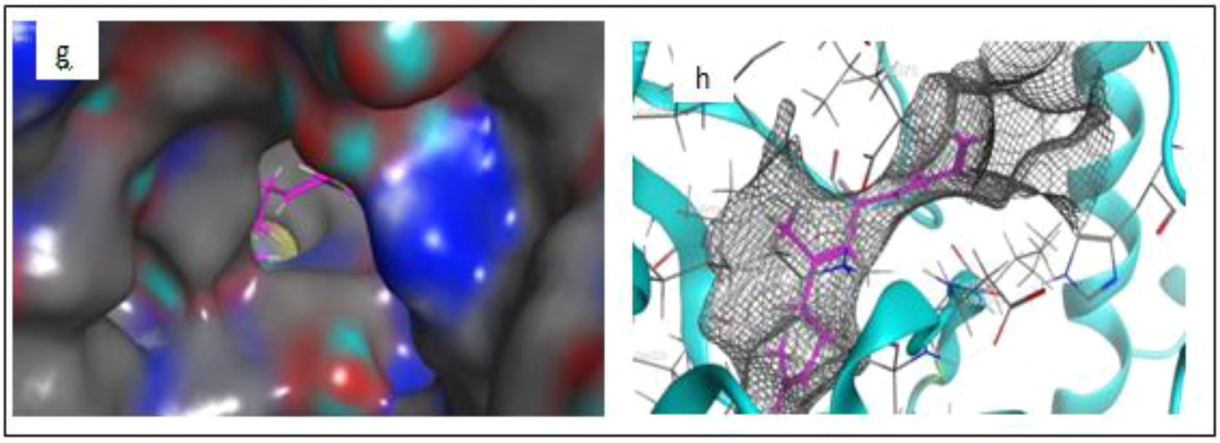

Figure 9. (g) The top scoring compound. (h) A novel inhibitor L-4 identified by molecular docking (*E*)-β-Farnesene is shown in the active site.

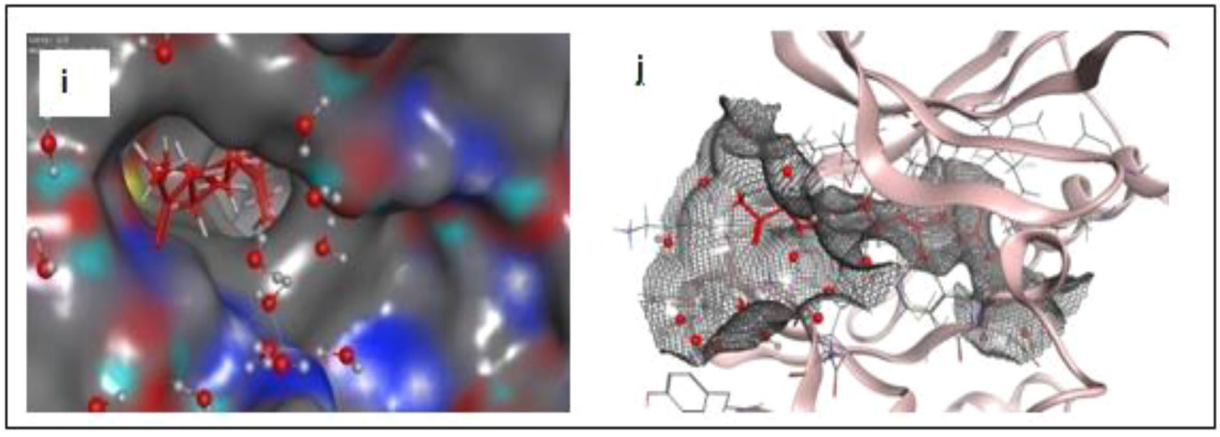

Figure 10. (i) The top scoring compound. **(j)** A novel inhibitor L-19 identified by molecular docking Farnesylacetoneis shown in the active site.

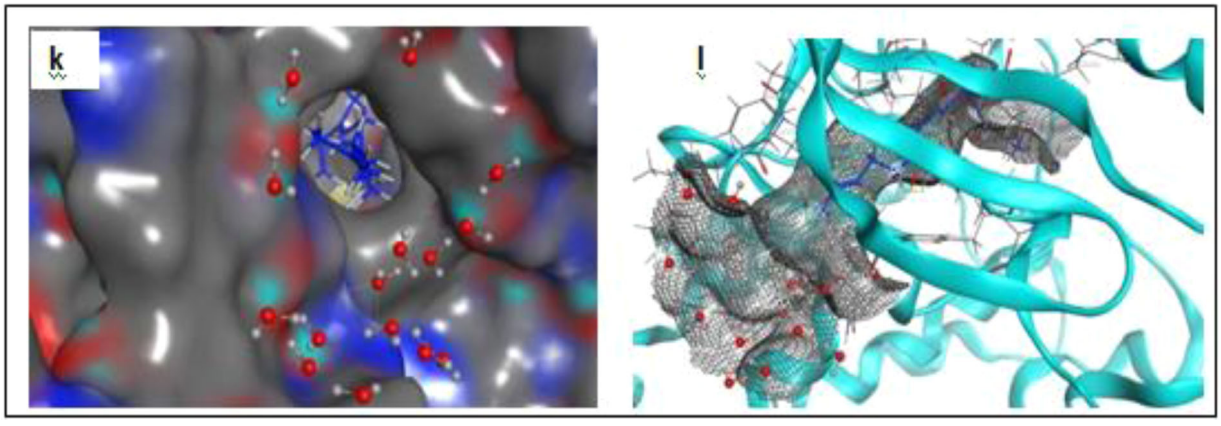

Figure 11. (k) The top scoring compound. **(l)** A novel inhibitor L4 identified by molecular docking (*E*)-β-Farneseneis shown in the active site.

the ligand L19, the amino acid residues NE and NH_2 at the N-terminal level of the α1 helix of VEGF were strongly involved in the interaction with the d2 domain of VEGFR1 (see Table 7).

4.4. MD

Using the MD simulation approach, we have studied the evolution thermodynamic properties of the ligand of complex 19 in NVT ensemble (Table 8).

For the ligand L19 in the VEGF enzyme and the VEGR1 receptor, the kinetic energies of translation and the internal energy were low compared to the VEGR2 receptors and the fluctuation in pressure for the VEGR2 receiver was significant. In contrast to the complex formed by L19 for the VEGF enzyme, the VEGR1 receptor was low. Canonical ensemble (NVT): moles (N), volume (V) and temperature (T) are conserved in simulation by molecular dynamic. Therefore, L19 was predicted to be the most interactive system. These results are in total agreement with the Docking prediction results (see Tables 5–7). We have shown the

Table 6. Results of bonds without water between atoms of best compounds and residues of the active site.

		Bonds between atoms of compounds and residues of the active site					
Compounds	S-score (kcal/mol)	**Atom of compound**	**Involved Receptor Atoms**	**Involved Receptor residues**	**Type of interaction bond**	**Distances (Å)**	**Energies (kcal/mol**
VEGF							
Lref1	−3.78999758	O3 21	ND2	ASN 75	H-acceptor	2.95	−0.7
L2	−3.54622912	O1 1	O	GLU 93 GLU 93	H-donor	2.51	1.2
					H-acceptor	2.82	
		O1 1	N				−1.0
L11	−3.98458982	O1 1	O	GLU 38	H-donor	2.58	−1.4
L12	−3.59765863	O1 1	N	LEU 97	H-acceptor	2.96	−1.3
VEGFR1							
Lref2	−10.2159939	N9 12	OE2	GLU 878	H-donor H-	2.88	−4.3
					acceptor H-	2.79	
					acceptor pi-H	2.81	
						3.86	
		O8 15	N	ASP 1040			−3.9
		N22 36	N	CYS 912 LYS 861			−4.9
		6-ring	CE				−0.8
L3	−5.31909132	C10 10	6-ring	PHE 1041	H-pi	4.08	−0.7
L14	−5.34053659	O1 1	O	GLU 910 CYS 912	H-donor	2.49	1.8
					H-acceptor	2.49	
		O1 1	N				1.7
L19	−7.96668291	O1 1	NE	ARG 1021	H-acceptor	3.00	−4.5
				ARG 1021	H-acceptor	2.94	
		O1 1	NH2				−1.6
VEGFR2							
Lref3	−10.4227104	N28 3	OE2	GLU 885 HOH	H-donor H-donor	2.74	−4.2
		N29 50		3334 ASP 1046		2.62	
		O30				2.66	
						3.24	
		N27 35	O	CYS 919	H-acceptor		−6.1
			N		H-acceptor		−1.9
			N				−3.3
L1	−4.71330452	C2 2	6-ring	PHE 1047	H-pi	4.44	−0.7
L16	−5.5116353	O1 1	O	HOH	H-donor	2.51	0.5
				3159ASN 923	H-acceptor	3.26	
		O1 1	N				−0.5
L11	−6.22930002	O1 1	O	ASP 1046	H-donor	2.95	−0.8
L18	−6.22930002	C6 6	6-ring	PHE 1047	H-pi	4.44	−0.6

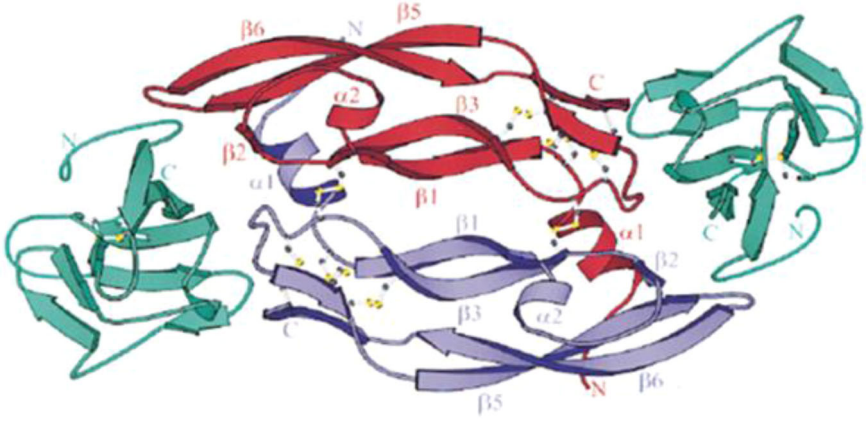

Figure 12. Structure of the VEGF / VEGFR1-d2 complex determined by X-ray crystallography. The VEGF dimer is represented in red and blue and the two VEGFR1-d2 domains in green (Ma et al., 2019).

detailed analysis of MD simulation results of only compound L19 with target VEGF receptors (Figures 13–15).

4.5. In silico assessment of the ADME

A computational study of two top scoring lead compounds was performed for the assessment of ADME properties and the obtained value is depicted in Table 9.

The results presented in Table 9 revealed that compound L19 has high absorption but compound L4 has low absorption. In addition, we can note that these compounds comply with Lipinski's rule of 5, Veber's rule and Egan's rule (Wiesmann et al., 1997), where log*P* values ranged between 4.50 and 4.84 (<5), MW range 204.35 − 262.43 (<500), HBA range 0 − 0 (≤ 10) and HBD range 0 − 0(<5), suggesting that these compounds would

Table 7. The docking energies of VEGF/VEGFR inhibitors.

Compound	Receptor	DE (kcal/mol)	ETOR (kT)	EVDW(kcal/mol	EIE (kcal/mol)
Lref1(Native)	VEGF	−3.78999758	446.407	1047540	−1737.84
Lref2 (Native)	VEGFR-1	−10.2159939	1368.097	2080.669	−5387.31
Lref3 (Native)	VEGFR-2	−10.4227104	1390.209	3828.302	−12968.3
cis-α-Bergamotene	VEGF	−3.49325585	1335.02	3562.36	−5425.32
	VEGFR-1	−5.67572975	1393.038	4147.532	−7697.59
	VEGFR-2	−4.71330452	1432.478	7939.513	−16668.8
(*E*)-β-Caryophyllene	VEGF	−3.54622912	433.400	1139.926	−2146.11
	VEGFR-1	−5.79094362	1385.513	4149.818	−7881.64
	VEGFR-2	−5.82724428	1410.691	7362.473	−16633.5
β-Copaene	VEGF	−3.38240385	427.554	1158.022	−2143.96
	VEGFR-1	−5.31909132	1389.996	5010.046	−7878.19
	VEGFR-2	−5.65643024	1407.077	532379.7	−16614.5
E)-β-Farnesene	VEGF	−4.01963854	414.741	2090.109	−2145.24
	VEGFR-1	−7.5542974	1359.000	4145.776	−7902.41
	VEGFR-2	−7.3946547	1392.285	6897.438	−16714.3
allo-Aromadendrene	VEGF	−3.38378692	430.065	1145.375	−2153.00
	VEGFR-1	−5.51163673	1371.339	231553.0	−7920.27
	VEGFR-2	−4.1189775	1443.131	6965.071	−16707.4
Germacrene-D	VEGF	−3.18338823	422.577	1307.654	−2170.70
	VEGFR-1	−5.51596737	1351.486	876706.2	−8017.91
	VEGFR-2	−5.33562517	1413.735	6276.327	−16765.2
Zingibrene	VEGF	−3.73947215	419.629	1557.475	−2169.54
	VEGFR-1	−6.2743659	1361.151	3623.325	−7950.19
	VEGFR-2	−6.0735530	1418.436	6344.492	−16807.0
Bicyclogermacrene	VEGF	−3.52705669	435.838	1161.354	−2167.69
	VEGFR-1	−4.31459522	1425.992	4574.672	−8036.23
	VEGFR-2	−5.7500782	1433.365	6378.849	−16813.3
γ-Cadinene	VEGF	−3.69257712	418.943	1173.223	−2176.87
	VEGFR-1	−5.35120869	1346.747	3704.720	−8035.35
	VEGFR-2	−5.50285721	1418.794	6395.554	−16875.6
δ-Cadinene	VEGF	−3.45229697	417.317	1176.686	−2181.88
	VEGFR-1	−5.29777861	1361.461	3664.779	−8029.96
	VEGFR-2	−5.40128326	1439.985	7144.735	−16887.5
(*E*)-Nerolidol	VEGF	−3.98458982	422.134	1164.999	−2186.37
	VEGFR-1	−6.78250837	1344.803	3657.513	−8052.21
	VEGFR-2	−6.5030674	1415.265	6451.999	−16925.8
Caryophyllene oxide	VEGF	−3.59765863	440.442	1168.931	−2181.25
	VEGFR-1	−5.14908934	1367.995	3668.767	−8032.72
	VEGFR-2	−5.5066609	1432.530	6516.935	−17038.0
Globulol	VEGF	−3.80335522	434.962	1154.406	−2180.96
	VEGFR-1	−4.79661131	1372.607	3671.807	−8054.30
	VEGFR-2	−5.6935491	1419.371	6517.878	−17007.6
Ledol	VEGF	−3.75419545	447.435	1172.155	−2193.51
	VEGFR-1	−5.34053659	1370.180	3672.611	−8060.27
	VEGFR-2	−5.68339872	1426.335	6473.761	−16958.5
Zingibereol	VEGF	−3.60531759	422.277	120516.4	−2201.03
	VEGFR-1	−5.08465052	1355.302	3664.348	−8048.25
	VEGFR-2	−5.73431635	1420.350	7133.076	−17031.6
τ-Muurolol	VEGF	−3.23660111	429.610	1175.279	−2180.06
	VEGFR-1	−5.04594994	1364.183	3653.479	−8038.35
	VEGFR-2	−5.5116353	1384.837	6176.431	−16669.6
α-Cadinol	VEGF	−3.55800462	428.868	1497.248	−2185.07
	VEGFR-1	−4.74857521	1360.631	3667.001	−8025.35
	VEGFR-2	−1.13416386	1403.009	6226.658	−16646.7
α-Bisabolol	VEGF	−3.71103525	424.113	1168.157	−2185.81
	VEGFR-1	−5.1971302	1350.979	3664.608	−8020.31
	VEGFR-2	−6.22930002	1389.838	6244.659	−16740.6
cis-α-Bergamotene	VEGF	−4.52469969	413.838	1568.082	−2164.04
	VEGFR-1	−7.96668291	1353.882	4156.540	−8033.24
	VEGFR-2	−8.10823059	1386.549	6252.439	−16605.2

DE: docking energy; ETOR: torsion energy; VDW: Van der Waals; EIE: electrostatic interaction energy.

not be expected to cause problems with oral bioavailability and thus showing possible utility of both compounds for developing the compound with good drug-like properties and in the meantime, we propose Ligand L19 Farnesylacetone present in essential oils of the aerial parts of *I. viscosa* with its proven activity score (−4.52469969, −7.96668291, −8.10823059), respectively, for VEGF, VEGFR-1, VEGFR-2 as a *new oral ligand* despite obeying Lipinski's rule.

4.6. Pharmacokinetics and medicinal chemistry properties

The results of Medicinal Chemistry and Pharmacokinetics showed that compound L19 has high GI absorptions but compound L4 has low GI absorptions. We notice that there is a correlation between our results for assessment of ADME properties (Table 9) and the predicted results in medicinal chemistry and pharmacokinetics (Table 10).

Table 8. Thermodynamic properties calculated in real units. Pressure $P = P^* \varepsilon/\sigma^{-3}$, energy of configuration $U = U^* N\varepsilon$, translation kinetic energy $EKT = EKT^* N\varepsilon$ and enthalpy $H = H^* N\varepsilon$.

SP_i	Method	H	U	EKT	P	V	T
SP_1	VEGF-Lig-19	−96.0353775	1507.44727	1388.18652	160.447647	12775.3398	357.959808
	VEGR1-Lig-19	−292.459259	3246.96533	4352.19336	−36.4663124	37559.7031	370.825592
	VEGR2-Lig-19	−346.652924	−1199.86816	4999.32471	−55.1730194	44492.7852	363.23175
	VEGR-Lig-19	−0.186085999	937.379517	1097.74744	−40.0676231	12775.3398	283.066742
	VEGR1-Lig-19	−7.79605532	2488.10181	4052.91699	183.276642	37559.7031	345.325989
	VEGR2-Lig-19	−0.443735003	−2920.92236	4110.30371	−254.836838	44492.7852	298.638916
	VEGR-Lig-19	0.175413504	959.181213	1135.01062	−58.5749931	12775.3398	292.675476
	VEGR1-Lig-19	0.186976507	1493.63403	3423.13843	93.5603485	37559.7031	291.666138
	VEGR2-Lig-19	1.34591353	−3326.87671	4023.22656	86.2301178	44492.7852	292.312225
SP_2	VEGR-Lig-19	0.323196739	926.048157	1186.59265	167.378677	12775.3398	305.976501
	VEGR1-Lig-19	0.186976507	1493.63403	3423.13843	93.5603485	37559.7031	291.666138
	VEGR2-Lig-19	1.34591353	−3326.87671	4023.22656	86.2301178	44492.7852	292.312225
	VEGR-Lig-19	−0.609911978	803.180115	1162.90198	−276.769501	12775.3398	299.867584
	VEGR1-Lig-19	−0.533955097	−0.805478334	3475.16797	39.4337997	37559.7031	296.099274
	VEGR2-Lig-19	−0.431310326	−3345.53491	4122.03809	43.8750153	44492.7852	299.491516
	VEGR-Lig-19	0.588058352	808.855286	1155.84644	132.805405	12775.3398	298.048248
	VEGR1-Lig-19	−0.527443051	1390.62939	3412.94312	−188.243103	37559.7031	290.797455
	VEGR2-Lig-19	1.69389367	−3485.01563	4041.8418	−1.55086923	44492.7852	293.664734
SP_3	VEGR-Lig-19	−0.239414528	832.668152	1137.39722	−119.197212	12775.3398	293.290924
	VEGR1-Lig-19	1.1400882	1405.06104	3494.96069	41.3016739	37559.7031	297.785706
	VEGR2-Lig-19	1.69389367	−3485.01563	4041.8418	−1.55086923	44492.7852	293.664734
	VEGR-Lig-19	0.697540104	853.860718	1097.72119	168.965363	12775.3398	283.059998
	VEGR1-Lig-19	1.57997549	1337.56262	3379.97607	117.144455	37559.7031	287.988525
	VEGR2-Lig-19	−1.35737085	−3514.72388	4062.38794	−46.1831398	44492.7852	295.157532
	VEGR-Lig-19	−0.016821704	1133.17383	1133.17383	124.116997	12775.3398	292.201874
	VEGR1-Lig-19	3.1954596	1367.98035	3419.4978	−95.8944092	37559.7031	291.355927
	VEGR2-Lig-19	1.8799262	−3460.46631	3998.78369	−149.61528	44492.7852	290.536285

Table 9. ADME properties for two top scoring lead compounds.

Entry	ABS	TPSA (Å^2)	n-ROTB	MW	MLog P	n-ON acceptors	n-OHNH donors	Lipinski's violations	Veber violations	Egan violations
Rule	–	–	–	<500	≤5	<10	<5	≤1	≤1	≤1
L4	Low	00.00	6	204.35	4.84	0	0	1	1	1
L19	High	17.07	9	262.43	4.50	1	0	1	1	1

ABS: absorption, TPSA: topological polar surface area, n-ROTB: number of rotatable bonds, MW: molecular weight, MLog*P*: logarithm of partition coefficient of compound between n-octanol and water, n-ON acceptors: number of hydrogen bond acceptors, n-OHNH donors: number of hydrogen bonds donors.

Table 10. Pharmacokinetics and medicinal chemistry properties for molecule scoring lead compounds.

		Pharmacokinetics			Medicinal chemistry	
N	Compounds	GI absorption	Log K_p (skin permeation)	Lipophilicity Log $P_{o/w}$ (MLOGP)	Lead-likeness	Synthetic accessibility
1	cis-α-Bergamotene	Low	−2.97 cm/s	4.63	No; 2 violations: $MW < 250$, XLOGP3 > 3.5	5.07
2	(*E*)-β-Caryophyllene	High	5.53 cm/s	3.56	No; 1 violation: MW < 250	4.48
3	β-Copaene	Low	5.65 cm/s	−4.37 cm/s	No; 2 violations: $MW < 250$, XLOGP3 > 3.5	4.62
4	(*E*)-β-Farnesene	Low	−3.20 cm/s	4.84	No; 2 violations: $MW < 250$, XLOGP3 > 3.5	3.72
5	allo-Aromadendrene	Low	−4.20 cm/s	5.65	No; 2 violations: $MW < 250$, XLOGP3 > 3.5	3.70
6	Germacrene-D	Low	−4.18 cm/s	4.53	No; 2 violations: $MW < 250$, XLOGP3 > 3.5	4.55
7	Zingibrene	Low	−3.88 cm/s	4.53	No; 2 violations: $MW < 250$, XLOGP3 > 3.5	4.81
8	Bicyclogermacrene	Low	−4.61 cm/s	4.63	No; 2 violations: $MW < 250$, XLOGP3 > 3.5	4.34
9	γ-Cadinene	Low	−4.85 cm/s	4.63	No; 2 violations: $MW < 250$, XLOGP3 > 3.5	4.14
10	δ-Cadinene	Low	−4.49 cm/s	4.63	No; 2 violations: $MW < 250$, XLOGP3 > 3.5	4.35
11	(*E*)-Nerolidol	High	−4.23 cm/s	3.86	No; 2 violations: $MW < 250$, XLOGP3 > 3.5	3.53
12	Caryophyllene oxide	High	−5.12 cm/s	3.67	No; 2 violations: $MW < 250$, XLOGP3 > 3.5	4.35
13	Globulol	High	−5.00 cm/s	3.81	No; 2 violations: $MW < 250$, XLOGP3 > 3.5	3.58
14	Ledol	High	−5.00 cm/s	3.81	No; 2 violations: $MW < 250$, XLOGP3 > 3.5	3.58
15	Zingibereol	High	−4.63 cm/s	3.56	No; 2 violations: $MW < 250$, XLOGP3 > 3.5	4.15
16	τ-Muurolol	High	−5.29 cm/s	3.67	No; 1 violation: MW < 250	4.29
17	α-Cadinol	High	−5.29 cm/s	3.67	No; 1 violation: MW < 250	4.29
18	α-Bisabolol	High	−4.97 cm/s	3.56	No; 2 violations: $MW < 250$, XLOGP3 > 3.5	3.95
19	*E*)-Z-Farnesylacetone	High	−3.95 cm/s	4.50	No; 2 violations: Rotors > 7, XLOGP3 > 3.5 MW < 350	3.47

(*E*)-Z-Farnesylacetone essential oils of the aerial parts of *I. viscosa* (oxygenated sesquiterpenes) (Ligand 19) was predicted to be characterized by a high lipophilicity and high coefficient of skin permeability log Kp by providing (*E*)-β-Farnesene (Ligand 4). We can resolve that the more negative the log Kp (with Kp in cm/s), the less the molecule is absorptive to the skin (Kacprzyk & Pedrycz, 2015), which explains the reliability of our results. We cite the works that

Table 11. Energy balance of complexes formed with VEGF under other experiments and our results for essential oils of *I. viscosa*.

Majority Molecule	Score	Reference
VEGF was received in the PDB database https://www.rcsb.org/) PDB ID: 5t89		
	VEGF	
Lref (Native)	−3.78999758	
Other experiments		
	VEGF	
(E)-nerolidol(19.8%) **Jordan**	−3.98458982	(Al-Qudah et al., 2010; Parikesit et al., 2015).
L-Bornéol (25.2%)	−3.23326421	
Bornylacetate(19.5%) **Turkey**	−3.47815251	(**Berendsen et al.**, 1984; Pérez-Alonso & Velasco-Negueruela, 1996).
Fokienol (21.1% et 38.8%, respectively) **France and Spain**	−4.01069689	(Blanc et al., 2006; Camacho et al., 2000; Parikesit et al., 2015; Pérez-Alonso & Velasco-Negueruela, 1996).
Acid Eudesma-3,11 (13) -dien-12-oïque (56.8%) and (62.4%, respectively) **Eastern Algeria and southern Italy**	−3.50546718	(Al-Qudah et al., 2010; Blanc et al., 2006; De Laurentis et al., 2002; Haoui et al., 2015).
δ-terpinene(35.9%) and α-pinene (18.9%) **Sidi Bel Abbes (Algeria)**	−3.20504832 −3.30435085	(Benchohra et al., 2011).
Acide isocostique (70.8%) **Tunisian**	−3.62129688	(Aissa et al., 2019; Benchohra et al., 2011).
isobutyrate de 3-méthoxy cuminyle(12%) **Portugal**	−4.26027393	(Mesli et al., 2019; Miguel et al., 2008).
Our Results		
(*E*)-Z-Farnesylacetone **L19** (13.2%) **Algeria**	−4.52469969	(Oxygenated sesquiterpenes)
(*E*)-β-Farnesene **L4** (2.6%) **Algeria**	−4.01963854	(Hydrocarbonsesquiterpene)

have proved the stability of complexes and their affinities by MOE software (Mesli et al., 2019; Mesli & Bouchentouf, 2018). Log $P_{o/w}$L19 > Log $P_{o/w}$L4 > Log $P_{o/w}$L11.

So Ligand L19 represents high affinity with VEGF receptors. Synthetic accessibility (SA) was a major factor to take into account in this selection process an acceptable value between 3.27and 3.47 for the ligands L19 and L4, respectively, and these are more promising molecules that can be synthesized or subjected to bioassays or other experiments. Our previous research has shown that oils from our region have better biological activities (Benyoucef et al., 2020; Miguel et al., 2008). Validation of our results, for essential oils of *I. viscosa*, in different region is mentioned in Table 11.

Our molecular docking results coincide with our experimental results; the oxygenated sesquiterpenes were the most dominant with a percentage of 87.3%.

Our ligand (E) -Z-Farnesylacetone (13.2%) better stabilizes the system with its energy of −4.52469969 Kcal/mol we compare with the components of other regions of the world (see Table 11). The latter allows good stabilization and complementarity of the complex. It is validated as a major ligand against cell cancer. The present molecular docking analysis MD simulations used to investigate new oxygenated sesquiterpene compound inhibitor of VEGF receptors. Previous studies have shown that (2Z,6E)-farnesol exhibited cytotoxic activity against human colon, liver and lung cancer cells (Cavalieri et al., 2004).

The ligands (*E*)-Z-Farnesylacetone inhibitor 19 and (*E*)-β-Farnesene (Ligand 4) we found are from the same family as (2Z,6E)-farnesol. The latter has good affinities to the VEGF receptors, which brings us back to the conclusion that the family oxygenated sesquiterpene was effective VEGF anti-angiogenic drugs.

In vitro, many studies were focused on the inhibitory effect of *I. viscosa* and nanobodies, on key enzymes linked to cancer therapy, VEGF receptors. Anti-VEGF NB strongly inhibits the migration of human endothelial cells ($p = 0.045$) (Kazemi-Lomedasht et al., 2017). Anti-VEGF NB significantly inhibits tumor growth in tumor-bearing mice ($p = 0.001$). Results indicate that NBs that are a novel class of antibodies derived from the camel can develop as a promising candidate for cancer drugs. The cross-reactive cross-linked NB showed high specificity and binding affinity in the nanomolar range for both human and mouse VEGF. In the case of anticancer activity, the American National Cancer Institute assigns a significant cytotoxic effect of promising anticancer products for future bioguided studies if IC_{50} value is lower than 30 μg/mL (Seca et al., 2014). According to Merghoub et al. (2009), the IC_{50} value greater than 54 μg/mL 'identifies a tumor effect'. For the same anticancer activity, IC_{50} values greater than 200 μg/mL (Mazzio & Soliman, 2009) are unacceptable. Talib and Mahasneh (2010) and Ferrara et al. (2004) found that *I. viscosa* flower extracts present low toxicity toward normal human cells (Vero cell line IC_{50} 202.43 ± 73.70 μg/mL). For *Inulaviscosa*, the IC_{50} values

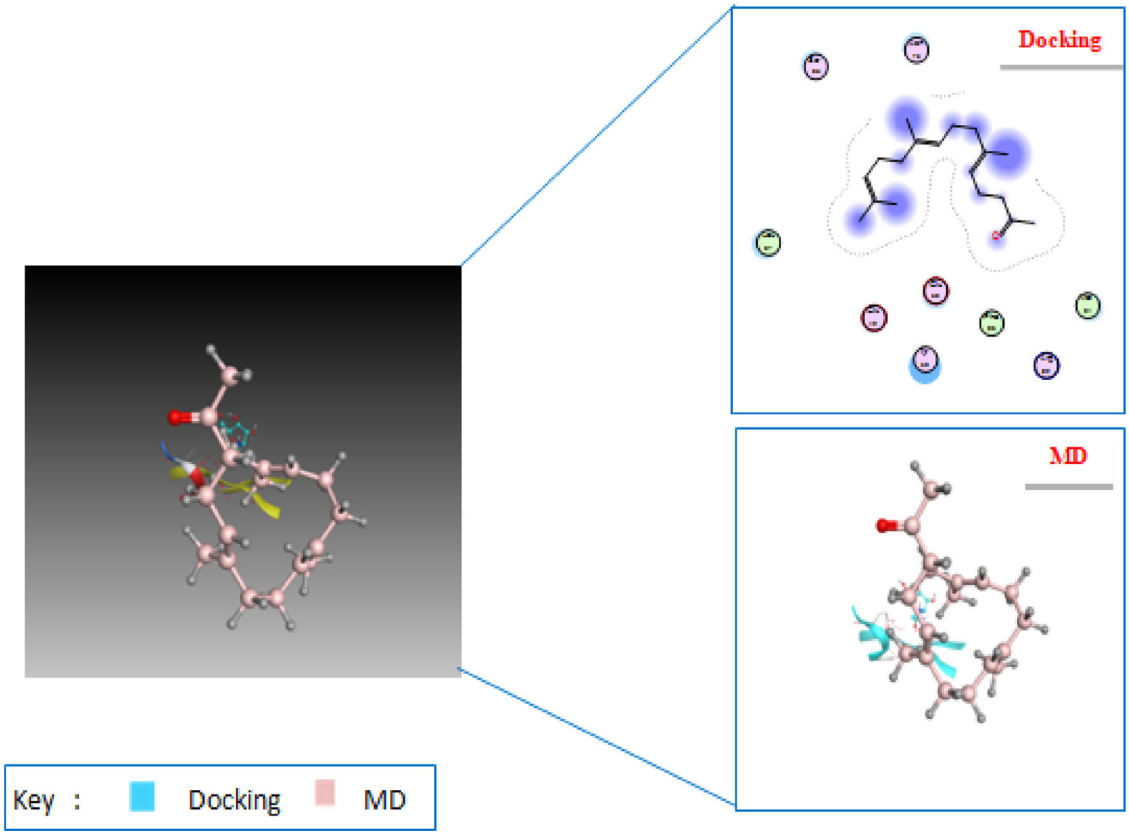

Figure 13. The compound – 19 Farnesylacetone is docked without water well into the binding site of **VEGF** and has the highest dock score; there is also a clear difference between the final ligand pose and the docking pose after a molecular dynamics (MD) simulation.

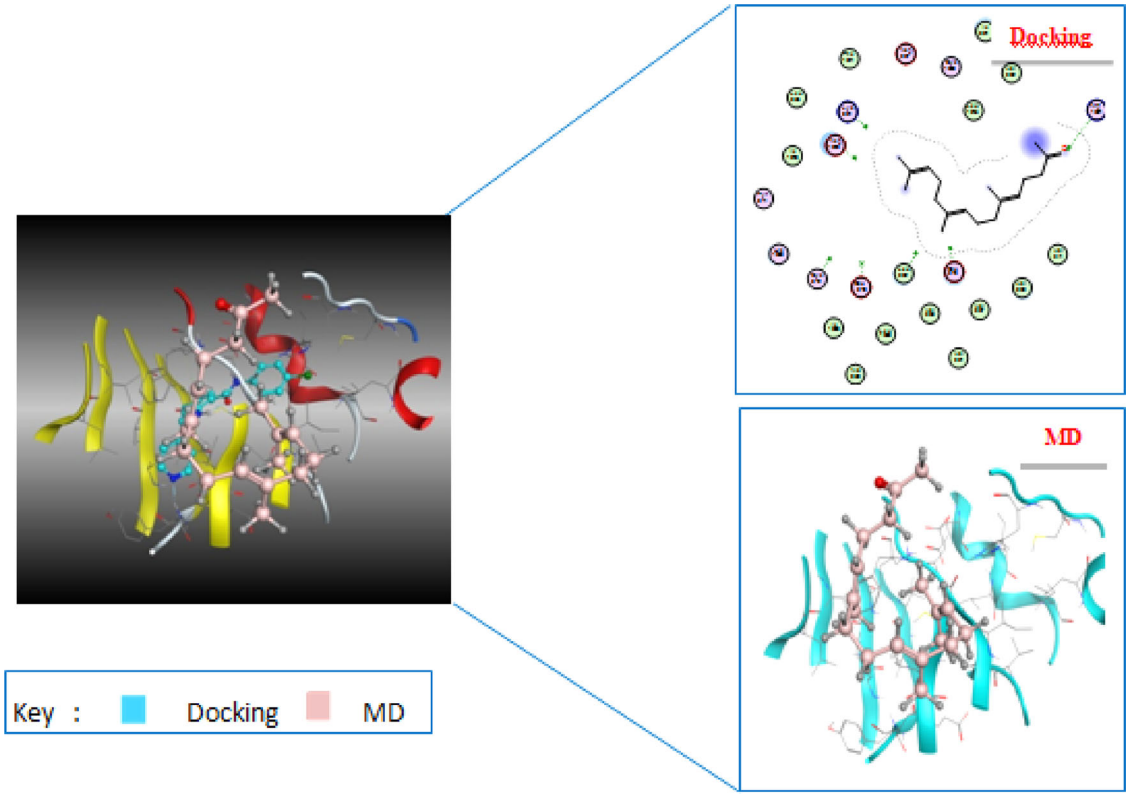

Figure 14. The compound – 19 Farnesylacetone is docked without water well into the binding site of VEGFR-1 and has the highest dock score; there is also a clear difference between the final ligand pose and the docking pose after a molecular dynamics (MD) simulation.

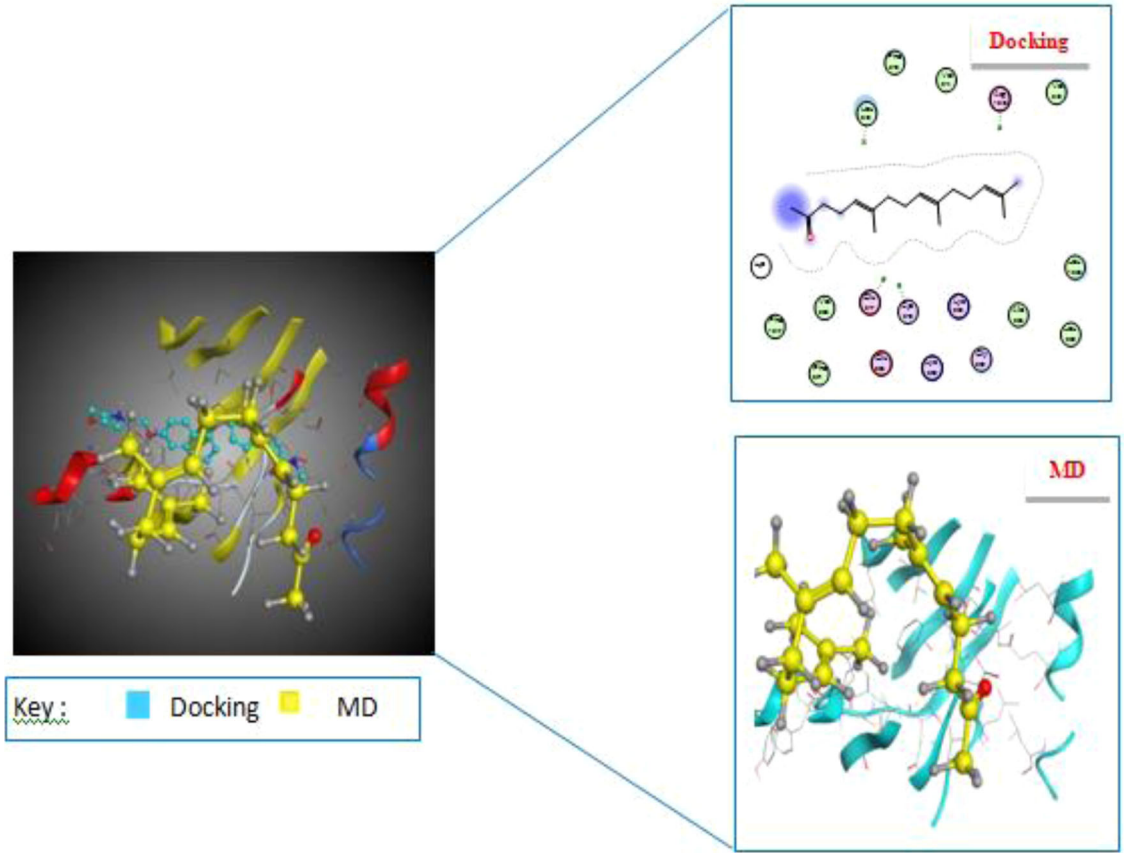

Figure 15. The compound – 19 Farnesylacetone is docked without water well into the binding site of VEGR-2 and has the highest dock score; there is also a clear difference between the final ligand pose and the docking pose after a molecular dynamics (MD) simulation.

recorded were in most cases 30 µg/mL. In addition, this sesquiterpene lactone from *Inulaviscosa* has anti-inflammatory activity according to several researchers (Hernández et al., 2001; Máñez et al., 2007;). In our case, the software package (*MOE*) does not identify any trace of the hydrophobic interactions between (*E*)-Z-Farnesylacetone and both theVEGF receptors, which may be related to the large size of this ligand and the high number of torsion angles (flexibility). The results are identified to have inhibitory activities against novel VEGF receptors. Of these compounds, (E)-Z-Farnesylacetone has a stronger bond and high affinity with VEGF. Therefore, the results obtained in this research honor ancestral know-how and provide real scientific support for the use of these plants by herbalists and traditional healers, while offering an imminent starting point for several studies to come.

5. Conclusion

The essential oil yield of *I. viscosa* showed a significant variability. Results showed the positive correlations between essential oil oxygenated sesquiterpene components and geographical locations. These compounds have been widely studied as VEGF inhibitors, which is of potential alternative drugs for the treatment of cancerous cells. Molecular docking used to study interaction between new compounds and VEGF receptors with score energy investigation and druglikeness properties experiments, ADME/T tests, Molecular dynamics simulation have been performed to verify in silico the drug properties of the top ligand (of essential oils of the aerial parts of the *I. viscosa*). The best ligand (*E*)-Z-Farnesylacetone which is the major componen, in of essential oils of the aerial parts of the I. viscosa) has high binding affinity (Score) and good substitution for ATP, thus preventing phosphorylation activity. The natural inhibitor – (*E*)-Z-Farnesylacetone – established different interactions between H-pi and H-acceptor with key residues for active site of targets. These results allow us to propose (*E*)-Z-Farnesylacetone natural and reliable treatment during the first stage of cancerous cells. Further *in vivo* and clinical studies regarding oxygenated sesquiterpenes to use as a useful supplementary agent in the pre-treatment of cancer are highly recommended.

Disclosure statement

The authors declare no conflict of interest.

Funding

Algerian Ministry of Higher Education and Scientific ResearchThe authors thanks the Algerian Ministry of Higher Education and Scientific Research for the support under the PRFU project (approval No. B00L01UN130120190009) and (approval No. BOOL01UN130120180004). The authors thank director of Laboratory -LASNABIO for his financial support. This research received no external funding.

References

Aissa, I., Nimbarte, V. D., Zardi-Bergaoui, A., Znati, M., Flamini, G., Ascrizzi, R., & Jannet, H. B. (2019). Isocostic acid, a promising bioactive agent from the essential oil of *Inula viscosa* (L.): Insights from drug likeness properties, molecular docking and SAR analysis. *Chemistry & Biodiversity*, *16*(4), e1800648. https://doi.org/10.1002/cbdv.201800648

Al-Dissi, N. M., Salhab, A. S., & Al-Hajj, H. A. (2001). Effects of *Inula viscosa* leaf extracts on abortion and implantation in rats. *Journal of Ethnopharmacology*, *77*(1), 117–121. https://doi.org/10.1016/S0378-8741(01)00261-6

Al-Hader, A., Aqel, M., & Hasan, Z. (1993). Hypoglycemic effects of the volatile oil of Nigella sativa seeds. *International Journal of Pharmacognosy*, *31*(2), 96–100. https://doi.org/10.3109/13880209309082925

Al-Qudah, M. A., Al-Jaber, H. I., Mayyas, A. S., Abu-Orabi, S. T., & Abu Zarga, M. H. (2010). Chemical compositions of the essential oil from the jordanian medicinal plant *Dittrichiaviscosa*. *Jordan Journal of Chemistry*, *5*, 343–348.

Arruebo, M., Vilaboa, N., Sáez-Gutierrez, B., Lambea, J., Tres, A., Valladares, M., & González-Fernández, Á. (2011). Assessment of the evolution of cancer treatment therapies. Cancers, *3*(3), 3279–3330. https://doi.org/10.3390/cancers3033279

Balusamy, S. R., Perumalsamy, H., Huq, M. A., & Balasubramanian, B. (2018). Anti-proliferative activity of *Origanum vulgare* inhibited lipogenesis and induced mitochondrial mediated apoptosis in human stomach cancer cell lines. *Biomedicine & Pharmacotherapy = Biomedecine & Pharmacotherapie*, *108*, 1835–1844. https://doi.org/10.1016/j.biopha.2018.10.028

Belabbes, R., Dib, M. E. A., Djabou, N., Ilias, F., Tabti, B., Costa, J., & Muselli, A. (2017). Chemical variability, antioxidant and antifungal activities of essential oils and hydrosol extract of *Calendula arvensis* L. from western Algeria. *Chemistry & Biodiversity*, *14*(5), e1600482. https://doi.org/10.1002/cbdv.201600482

Benchohra, H. A., Hamel, L., Bendimered, F. Z., & Benchohra, M. (2011). Chemical composition of essential oil of *Inula viscosa*. *Science Lib*, *3*, 1–6.

Benyoucef, F., Dib, M. E., Tabti, B., Zoheir, A., Costa, J., & Muselli, A. (2020). Synergistic effects of essential oils of *Ammoides verticillata* and *Satureja candidissima* against many pathogenic microorganisms. *Anti-Infective Agents*, *18*(1), 72–78. https://doi.org/10.2174/2211352517666190227161811

Berendsen, H. J., Postma, J. V., van Gunsteren, W. F., DiNola, A. R. H. J., & Haak, J. R. (1984). Molecular dynamics with coupling to an external bath. *The Journal of Chemical Physics*, *81*(8), 3684–3690. https://doi.org/10.1063/1.448118

Blanc, M. C., Bradesi, P., Gonc¸Alves, M. J., Salgueiro, L., & Casanova, J. (2006). Essential oil of *Dittrichia viscosa* spp. *viscosa*: Analysis by 13C-NMR and antimicrobial activity. *Flavour and Fragrance Journal*, *21*(2), 324–332.

Bond, S. D., Leimkuhler, B. J., & Laird, B. B. (1999). The Nosé–Poincaré method for constant temperature molecular dynamics. *Journal of Computational Physics*, *151*(1), 114–134. https://doi.org/10.1006/jcph.1998.6171

Bouyahya, A., Et-Touys, A., Khouchlaa, A., El-Baaboua, A., Benjouad, A., Amzazi, S., Dakka, N., & Bakri, Y. (2018). Notes ethnobotaniques et phytopharmacologiques sur *Inula viscosa*. *Phytothérapie*. https://doi.org/10.1007/s10298-017-1176-2.

Cafarchia, C., De Laurentis, N., Milillo, M. A., Losacco, V., & Puccini, V. (2002). Antifungal activity of essential oils from leaves and flowers of *Inula viscosa* (Asteraceae) by Apulian region. Parassitologia, *44*(3–4), 153–156.

Camacho, A., Fernandez, A., Fernandez, C., Altarejos, J., & Laurent, R. (2000). Composition of the essential oil of *Dittrichia viscosa* (L.) W. Greuter. *Rivista Italiana*, *29*, 3–8. https://www.cabdirect.org/cabdirect/abstract/20000312872

Cavalieri, E., Mariotto, S., Fabrizi, C., de Prati, A. C., Gottardo, R., Leone, S., Berra, L. V., Lauro, G. M., Ciampa, A. R., & Suzuki, H. (2004). alpha-Bisabolol, a nontoxic natural compound, strongly induces apoptosis in glioma cells. *Biochemical and Biophysical Research Communications*, *315*(3), 589–594. https://doi.org/10.1016/j.bbrc.2004.01.088

Chahmi, N., Anissi, J., Jennan, S., Farah, A., Sendide, K., & El Hassouni, M. (2015). Antioxidant activities and total phenol content of *Inulaviscosa* extracts selected from three regions of Morocco. *Asian Pacific Journal of Tropical Biomedicine*, *5*(3), 228–233. https://doi.org/10.1016/S2221-1691(15)30010-1

Champagnat, M. N., Talay, M. D., & Perrin, N. (2013). Méthodes stochastiques en dynamique moléculaire. Université Nice-Sophia Antipolis.

Chiarlo, B. (1968). On the constituents of Inula viscosa Ait. I. Essential oil content of azulenes. *Bollettino Chimico Farmaceutico*, *107*(6), 370. PMID: 4182546

Daina, A., Michielin, O., & Zoete, V. (2017). SwissADME: A free web tool to evaluate pharmacokinetics, drug-likeness and medicinal chemistry friendliness of small molecules. *Scientific Reports*, *7*, 42717. https://doi.org/10.1038/srep42717

De Laurentis, N., Losacco, V., Milillo, M. A., & Lai, O. (2002). Chemical investigations of volatile constituents of *Inulaviscosa* (L) Aiton (Asteraceae) from different areas of Apulia, Southern Italy. *Delpinoa, n.s*, *44*, 115–119.

Haoui, I. E., Derriche, R., Madani, L., & Oukali, Z. (2015). Analysis of the chemical composition of essential oil from Algerian *Inula viscosa* (L.) Aiton. *Arabian Journal of Chemistry*, *8*(4), 587–590. https://doi.org/10.1016/j.arabjc.2011.05.005

Hernández, V., del Carmen Recio, M., Máñez, S., Prieto, J. M., Giner, R. M., & Ríos, J. L. (2001). A mechanistic approach to the in vivo anti-inflammatory activity of sesquiterpenoid compounds isolated from Inula viscosa. *Planta Medica*, *67*(8), 726–731. https://doi.org/10.1055/s-2001-18342

Hou, C. J., Kulka, M., Zhang, J. Z., Li, Y. M., & Guo, F. J. (2014). Occurrence and biological activities of eremophilane-type sesquiterpenes. *Mini Reviews in Medicinal Chemistry*, *14*(8), 664–677. https://doi.org/10.2174/1389557514666140820105422

Jennings, W., & Shibamoto, T. (1980). *Qualitative analysis of flavour and fragrance volatiles by glass-capillary gas chromatography*. H. B. Jovanovich (Ed.) (1st ed.). Academic Press.

Joulain, D., & König, W. A. J. (1998). *The atlas of spectra data of sesquiterpene hydrocarbone*. EB-Verlag.

König, W. A., Hochmuth, D. H., & Joulain, D. (2001). *Terpenoids and related constituents of essential oils, library of mass finder 2.1*. Hamburg: Institute of Organic Chemistry, University of Hamburg.

Kacprzyk, J., & Pedrycz, W. (Eds.). (2015). *Springer handbook of computational intelligence*. Springer.

Kazemi-Lomedasht, F., Pooshang-Bagheri, K., Habibi-Anbouhi, M., Hajizadeh-Safar, E., Shahbazzadeh, D., Mirzahosseini, H., & Behdani, M. (2017). *In vivo* immunotherapy of lung cancer using cross-species reactive vascular endothelial growth factor nanobodies. *Iranian Journal of Basic Medical Sciences*, *20*(5), 489–496. https://doi.org/10.22038/IJBMS.2017.8672

Khana, A., Khana, H., & Hussaina, J. (2008). Sesquiterpenes: The potent antioxidants. Pakistan *Journal of Scientific and Industrial Research*, *51*(6), 343–350. https://v2.pjsir.org/index.php/biological-sciences/article/view/711

Lauro, L., & Rolih, C. (1990). Observations and research on an extract of Inula viscosa Ait. *Bollettino Della Societa Italiana di Biologia Sperimentale*, *66*(9), 829. PMID: 2073383

Lipinski, C. A., Lombardo, F., Dominy, B. W., & Feeney, P. J. (1997). Experimental and computational approaches to estimate solubility and permeability in drug discovery and development settings. *Advanced drug delivery reviews*, *23*(1–3), 3–25. https://doi.org/10.1016/j.addr.2012.09.019

Lesgards, J. F., Baldovini, N., Vidal, N., & Pietri, S. (2014). Anticancer activities of essential oils constituents and synergy with conventional therapies: A review. *Phytotherapy Research: Ptr*, *28*(10), 1423–1446. https://doi.org/10.1002/ptr.5165

Ma, G.-H., Chen, K.-X., Zhang, L.-Q., & Li, Y.-M. (2019). Advance in biological activities of natural guaiane-type sesquiterpenes. *Medicinal Chemistry Research*, *28*(9), 1339–1358. https://doi.org/10.1007/s00044-019-02385-7

Máñez, S., Hernández, V., Giner, R. M., Ríos, J. L., & del Carmen Recio, M. (2007). Inhibition of pro-inflammatory enzymes by inuviscolide, a sesquiterpene lactone from Inula viscosa. Fitoterapia, *78*(4), 329–331. https://doi.org/10.1016/j.fitote.2007.03.005

Mazzio, E. A., & Soliman, K. F. (2009). *In vitro* screening for the tumoricidal properties of international medicinal herbs. *Phytotherapy Research: An International Journal Devoted to Pharmacological and Toxicological Evaluation of Natural Product Derivatives*, *23*(3), 385–398. https://doi.org/10.1002/ptr.2636

Mc Lafferty, F. W., & Stauffer, D. B. (1988). *The Wiley/NBS Registry of Mass Spectra Data* (1st ed.). Wiley-Interscience.

Merghoub, N., Benbacer, L., Amzazi, S., Morjani, H., & El-Mzibri, M. (2009). Cytotoxic effect of some Moroccan medicinal plant extracts on human cervical cell lines. *Journal of Medicinal Plants Research*, *3*(12), 1045–1050. https://doi.org/10.5897/JMPR.9000424

Mesli, F., & Bouchentouf, S. (2018). PREDICTION OF STRUCTURAL AND THERMODYNAMIC PROPERTIES OF CHROMEN USING NUMERICAL METHODS. *Pharmacophore*, *9*(4), 14–20. https://orcid.org/10.7324/JAPS.2019.90104

Mesli, F., Daoud, I., & Ghalem, S. (2019). ANTIDIABETIC ACTIVITY OF NIGELLA SATIVA (BLACK SEED)-BY MOLECULAR MODELING ELUCIDATION, MOLECULAR DYNAMIC, AND CONCEPTUAL DFT INVESTIGATION. *Ene*, *17868*(136.2380), C10H16. http://www.pharmacophorejournal.com

Miguel, G., Faleiro, L., Cavaleiro, C., Salgueiro, L., & Casanova, J. (2008). Susceptibility of *Helicobacter pylori* to essential oil of *Dittrichia viscosa* subsp. *revoluta*. *Phytotherapy Research: Ptr*, *22*(2), 259–263. https://doi.org/10.1002/ptr.2284

Molecular Operating Environment (MOE), *2013.08*. (2016). Chemical Computing Group Inc., 1010 Sherbooke St. West, Suite #910, Montreal, QC, Canada, H3A 2R7, *2019*.

National Institute of Standards and Technology. (2008). NIST ChemistryWebBook, NIST Standard Reference Database, Gaisthersburg, MD. http://webbook.nist.gov/chemistry

Nisha, C. M., Kumar, A., Nair, P., Gupta, N., Silakari, C., Tripathi, T., & Kumar, A. (2016). Molecular docking and *in silico* ADMET study reveals acylguanidine 7a as a potential inhibitor of β-secretase. *Advances in Bioinformatics*, *2016*, 9258578.

Novelli, G. P. (1997). Role of free radicals in septic shock. *Journal of Physiology and Pharmacology: An Official Journal of the Polish Physiological Society*, *48*(4), 517–527. PMID: 9444605

Parikesit, A. A., Nugroho, A. S., Hapsari, A., & Tambunan, U. S. F. (2015). The Computation of cyclic peptide with prolin-prolin bond as fusion inhibitor of DENV envelope protein through molecular docking and molecular dynamics simulation. *arXiv preprint arXiv:1511.01388*.

Pérez-Alonso, M. J., Velasco-Negueruela, A., Duru, M. E., Harmandar, M., & García Vallejo, M. C. (1996). Composition of the volatile oil from the aerial parts of *Inulaviscosa* (L) Aiton. *Flavour and Fragrance Journal*, *11*(6), 349–351.

Petersson, A., Bennett, A., Tensfeldt, T. G., Al, -Laham, M. A., Shirley, W. A., & Mantzaris, J. (1988). A complete basis set model chemistry. I. The total energies of closed-shell atoms and hydrides of the first-row elements. *The Journal of Chemical Physics*, *89*(4), 2193–2218. https://doi.org/10.1063/1.455064

Rasouli, H., Hosseini-Ghazvini, S. M.-B., Adibi, H., & Khodarahmi, R. (2017). Differential α-amylase/α-glucosidase inhibitory activities of plant-derived phenolic compounds: A virtual screening perspective for the treatment of obesity and diabetes. *Food & Function*, *8*(5), 1942–1954. https://doi.org/10.1039/c7fo00220c

Rozenblat, S., Grossman, S., Bergman, M., Gottlieb, H., Cohen, Y., & Dovrat, S. (2008). Induction of G2/M arrest and apoptosis by sesquiterpene lactones in human melanoma cell lines. *Biochemical Pharmacology*, *75*(2), 369–382. https://doi.org/10.1016/j.bcp.2007.08.024

Salim, B., Hocine, A., & Said, G. (2017). First study on anti-diabetic effect of rosemary and salvia by using molecular docking. *Journal of Pharmaceutical Research International*, *19*(4), 1–12. https://doi.org/10.9734/JPRI/2017/37061

Seca, A. M., Grigore, A., Pinto, D. C., & Silva, A. M. (2014). The genus *Inula* and their metabolites: From ethnopharmacological to medicinal uses. *Journal of Ethnopharmacology*, *154*(2), 286–310. https://doi.org/10.1016/j.jep.2014.04.010

Sturgeon, J. B., & Laird, B. B. (2000). Symplectic algorithm for constant-pressure molecular dynamics using a Nosé–Poincaré thermostat. *The Journal of Chemical Physics*, *112*(8), 3474–3482. https://doi.org/10.1063/1.480502

Su, Y.-C., Hsu, K.-P., Wang, E. I.-C., & Ho, C.-L. (2015). Composition, in vitro cytotoxic, and antimicrobial activities of the flower essential oil of diospyros discolor from Taiwan. *Natural Product Communications*, *10*(7), 1934578X1501000.

Talib, W. H., & Mahasneh, A. M. (2010). Antiproliferative activity of plant extracts used against cancer in traditional medicine. *Scientia Pharmaceutica*, *78*(1), 33–46. https://doi.org/10.3797/scipharm.0912-11

Talib, W. H., & Mahasneh, A. M., (2010). Antimicrobial, cytotoxicity and phytochemical screening of Jordanian plants used in traditional medicine. *Molecules (Basel, Switzerland)*, *15*(3), 1811–1824.33.

Ferrara, N., Hillan, K. J., Gerber, H. P., & Novotny, W. (2004). Discovery and development of bevacizumab, an anti-VEGF antibody for treating cancer. *Nature Reviews Drug Discovery*, *3*, 391–400. https://doi.org/10.3390/molecules15031811

Talib, W. H., Zarga, M. H. A., & Mahasneh, A. M. (2012). Antiproliferative, antimicrobial and apoptosis inducing effects of compounds isolated from Inula viscosa. *Molecules (Basel, Switzerland)*, *17*(3), 3291–3303. https://doi.org/10.3390/molecules17033291

Tresaugues, L., Roos, A., Arrowsmith, C., Berglund, H., Bountra, C., & Collins, R. (2013). Crystal structure of VEGFR1 in complex with N-(4-chlorophenyl)-2-((pyridin-4-ylmethyl) amino) benzamide. *The RCSB PDB*. https://doi.org/10.2210/pdb3HNG/pdb

Walker, C. B. (1996). The acquisition of antibiotic resistance in the periodontal microflora. *Periodontology 2000*, *10*(1), 79–88. https://doi.org/10.1111/j.1600-0757.1996.tb00069.x

Wiesmann, C., Fuh, G., Christinger, H. W., Eigenbrot, C., Wells, J. A., & deVos, A. M. (1997). Crystal structure at 1.7 Å resolution of VEGF in complex with domain 2 of the Flt-1 receptor. *Cell*, *91*, 695–704. https://doi.org/10.1016/S0092-8674(00)80456-0